Human Molecular Genetics, 2010, Vol. 19, No. 9 **1633–1650**
doi:10.1093/hmg/ddq038
Advance Access published on January 27, 2010

Extensive enteric nervous system abnormalities in mice transgenic for artificial chromosomes containing Parkinson disease-associated α-synuclein gene mutations precede central nervous system changes

Yien-Ming Kuo[1], Zhishan Li[3], Yun Jiao[4], Nathalie Gaborit[5], Amar K. Pani[4], Bonnie M. Orrison[6], Benoit G. Bruneau[5], Benoit I. Giasson[7], Richard J. Smeyne[4], Michael D. Gershon[3] and Robert L. Nussbaum[1,2,*]

[1]Department of Medicine and [2]Institute for Human Genetics, University of California San Francisco, San Francisco, CA 94143, USA, [3]Department of Pathology and Cell Biology, Columbia University, New York, NY 10032, USA, [4]Department of Developmental Neurobiology, St. Jude Children's Research Hospital, Memphis, TN 38105, USA, [5]Gladstone Institute of Cardiovascular Disease, San Francisco, CA 94158, USA, [6]Genetic Disease Research Branch, NHGRI, National Institutes of Health, Bethesda, MD 20892, USA and [7]Department of Pharmacology, University of Pennsylvania School of Medicine, Philadelphia, PA 19104, USA

Received December 15, 2009; Revised and Accepted January 25, 2010

Parkinson disease (PD) is a neurodegenerative disease with motor as well as non-motor signs in the gastrointestinal tract that include dysphagia, gastroparesis, prolonged gastrointestinal transit time, constipation and difficulty with defecation. The gastrointestinal dysfunction commonly precedes the motor symptoms by decades. Most PD is sporadic and of unknown etiology, but a fraction is familial. Among familial forms of PD, a small fraction is caused by missense (A53T, A30P and E46K) and copy number mutations in *SNCA* which encodes α-synuclein, a primary protein constituent of Lewy bodies, the pathognomonic protein aggregates found in neurons in PD. We set out to develop transgenic mice expressing mutant α-synuclein (either A53T or A30P) from insertions of an entire human *SNCA* gene as models for the familial disease. Both the A53T and A30P lines show robust abnormalities in enteric nervous system (ENS) function and synuclein-immunoreactive aggregates in ENS ganglia by 3 months of age. The A53T line also has abnormal motor behavior but neither demonstrates cardiac autonomic abnormalities, olfactory dysfunction, dopaminergic neurotransmitter deficits, Lewy body inclusions or neurodegeneration. These animals recapitulate the early gastrointestinal abnormalities seen in human PD. The animals also serve as an *in vivo* system in which to investigate therapies for reversing the neurological dysfunction that target α-synuclein toxicity at its earliest stages.

INTRODUCTION

Parkinson disease (PD) is the second most common neurodegenerative disease after Alzheimer disease, with a prevalence in the USA of 0.3%, rising to 1.5% in the over 55 age group (1). PD affects the central nervous systems (CNS), peripheral nervous system (PNS) and enteric nervous systems (ENS). Loss of dopaminergic neurons of the substantia nigra pars compacta (SNpc) and their nigrostriatal projections produces parkinsonism, the movement disorder characterized by

*To whom correspondence should be addressed at: Box 0794 UCSF, 513 Parnassus Avenue, San Francisco, CA 94143, USA. Tel: +1 4154763200; Fax: +1 4155020720; Email: nussbaumr@humgen.ucsf.edu

tremor, bradykinesia, rigidity and postural instability that are the most obvious clinical signs of the disease (2–4). Non-motor abnormalities are also seen frequently in PD (5). These include depression, sleep disturbances, hyposmia and dementia with Lewy bodies, which result from lesions outside the SNpc but inside the CNS. Autonomic and gastrointestinal dysfunction are also common and are associated with pathological changes outside the CNS (6). Gastrointestinal dysfunction is a particularly common non-motor abnormality in PD, documented in over 80% of patients [Reviewed by Pfeiffer (7), Jost and Eckhart (8) and Jost (9)]. Symptoms and signs include dysphagia, gastroparesis, prolonged gastrointestinal transit time, constipation and difficulty with defecation (10). Gastrointestinal dysfunction precedes the onset of motor symptoms in PD patients by decades (11,12).

Cytoplasmic protein aggregates known as Lewy bodies, distributed throughout the CNS from the lower brainstem through the midbrain and forebrain and cerebral cortex, are pathological hallmarks of the disease (13,14). Aggregates of α-synuclein and Lewy bodies are also found in the ENS of PD patients (15–17). However, it remains unclear whether Lewy bodies are toxic, protective or neutral markers of the PD process.

Most cases of PD are sporadic and of unknown etiology. However, a small fraction are familial and caused by mutations in single genes (18). In particular, three different missense mutations (A53T, A30P and E46K) and various copy number mutations (duplication and triplication) in *SNCA*, the gene encoding α-synuclein, cause rare familial, highly penetrant autosomal dominant PD (19–23). Although familial forms of PD due to mutations in *SNCA* are rare, they are important for two reasons. First, α-synuclein is one of the primary protein constituents of Lewy bodies in all PD, including the sporadic forms (24–26). Second, many transgenic mouse models for PD have been made that rely on overexpression of human α-synuclein driven by heterologous promoters [Reviewed by Chesselet (27), Meredith *et al*. (28), Terzioglu and Galter (29) and Melrose *et al*. (30)]. We have developed two new lines of transgenic animals, each expressing one of two mutant forms of α-synuclein (A53T and A30P) from transgenic insertions of a bacterial artificial chromosome containing the entire human *SNCA* gene. We then crossed these onto a background of mice carrying a partial deletion of the mouse *Snca* gene that eliminates all expression of α-synuclein protein so that the only α-synuclein in these mice is the human protein. We have assessed these transgenic animals over 18–24 months for many of the motor and non-motor abnormalities found in PD. By 3 months of age, both the A53T and A30P lines of mice show robust abnormalities in ENS function whereas only the A53T line develops abnormal motor behavior without detectable non-enteric autonomic abnormalities, olfactory dysfunction or dopaminergic deficits, Lewy body inclusions or neurodegeneration. The early ENS dysfunction in the absence of major CNS pathology mimics what is seen early in human PD, where ENS dysfunction has been reported to precede the more classical motor symptoms by years to decades (7–9,31). These animals are models with which to identify the earliest abnormalities in neuronal function as well as the later pathogenic steps leading to nervous system degeneration in PD. Finally, the animals can also serve as an *in vivo* system that can be used to investigate approaches designed to reverse the neurological dysfunction induced by α-synuclein toxicity at its earliest stages.

RESULTS

Creating transgenic animals

We used recombineering in *Escherichia coli* (32) to introduce the A30P or A53T mutations into P1 artificial chromosome (PAC) RP1-27M07 containing the entire human *SNCA* gene by a two-step allelic exchange procedure. Clones in which the A30P or A53T mutation had been engineered into exon 3 and 4, respectively, were analyzed by restriction mapping and direct sequencing to demonstrate that the correct mutations had been introduced without causing rearrangements of the PACs (data not shown).

We set out to create five cohorts of mice. First, we generated transgenic mouse lines carrying either the $SNCA^{A53T}$ PAC or the $SNCA^{A30P}$ PAC as transgenes in FVB/N mice. These lines will be referred to as PAC-Tg($SNCA^{A53T}$) and PAC-Tg($SNCA^{A30P}$), respectively. Two independent lines of founder mice for each construct were chosen for further breeding based on their level of expression of the mutant α-synuclein and their ability to transmit the transgene in their germlines. Because our previous work with a prion promoter driven *SNCA* transgene indicated a more severe phenotype developed in mice in which the mouse *Snca* gene was deleted ($Snca^{-/-}$) (33), the two PAC-Tg($SNCA^{A53T}$) transgenic lines were crossed with $Snca^{-/-}$ knock-out mice, which are on a 129S6//SvEvTac background (34). Breeding was continued until we had generated mice homozygous for both the PAC-Tg($SNCA^{A53T}$) transgene and the *Snca* deletion [referred to as PAC-Tg($SNCA^{A53T}$)$^{+/+}$;$Snca^{-/-}$]. In order to increase expression levels of mutant α-synucleins to levels seen in families with duplication or triplication of the *SNCA* gene, the two PAC-Tg($SNCA^{A53T}$)$^{+/+}$;$Snca^{-/-}$ lines were crossed with each other and the resulting F1 generation intercrossed to generate double transgenic animals homozygous for both insertion sites of the $SNCA^{A53T}$ PAC [referred to as dbl-PAC-Tg($SNCA^{A53T}$)$^{+/+}$;$Snca^{-/-}$]. Similarly, double transgenic animals homozygous for both insertion sites of the $SNCA^{A30P}$ PAC in an $Snca^{-/-}$ background were also generated from the two independent PAC-Tg($SNCA^{A30P}$) lines (referred to as dbl-PAC-Tg($SNCA^{A30P}$)$^{+/+}$;$Snca^{-/-}$). However, because one of the $SNCA^{A30P}$ lines insertions was on the X chromosome, only female dbl-PAC-Tg($SNCA^{A30P}$)$^{+/+}$;$Snca^{-/-}$ had four copies of the $SNCA^{A30P}$ PAC whereas the males had three. Three control lines of a mixed FVB/N × 129S6/SvEvTac similar to the transgenic animals with mutant PAC *SNCA* transgenes were also generated. These were (i) mice homozygous for the wild-type human *SNCA* PAC transgene (PAC-Tg($SNCA^{WT}$)$^{+/+}$) (35) bred onto the $Snca^{-/-}$ background (34), (ii) *Snca* knock-out mice ($Snca^{-/-}$) crossed with wild-type FVB/N and (iii) wild-type 129S6/SvEvTac crossed with wild-type FVB/N. The resulting three control lines (PAC-Tg($SNCA^{WT}$)$^{+/+}$);$Snca^{-/-}$, $Snca^{-/-}$ and $Snca^{+/+}$ were used throughout our studies as controls.

SNCA expression

The expression of α-synuclein in total brain and descending colon in the control and mutant *SNCA* lines was measured relative to endogenous mouse *Snca* by quantitative PCR (qPCR) and by western blotting for α-synuclein protein. For qPCR, we calibrated *SNCA* or *Snca* expression against two different endogenous mouse neuronal gene standards, HuD antigen (*Elavl4*) and synaptophysin (*Syp*) (see Supplementary Material, Table S1 for details). We then calculated the relative expression of wild-type or mutant human *SNCA* transcript in female mice against endogenous mouse *Snca* using the $\Delta\Delta C_t$ method (Fig. 1). At 6 weeks of age, the PAC-Tg($SNCA^{WT}$)$^{+/+}$;$Snca^{-/-}$ line expressed wild-type human *SNCA* at ∼40-fold higher levels in brain compared with endogenous mouse *Snca* expression, although the two double-transgenic lines expressed between 8-fold and 21-fold more message. Western blot analysis of whole brain from 6 week (data not shown) to 6-month-old animals (Fig. 1B) revealed a modest increase in the amount of protein (1.3–2-fold) that was not proportional to the much greater transcript levels seen by qPCR. In the distal colon, all three transgenic lines contained two-to-three orders of magnitude more *SNCA* transcript compared with endogenous mouse *Snca*. In contrast, western blotting for α-synuclein in the colon of 6-month-old $Snca^{+/+}$ mice (Fig. 1B) showed only a faint band of endogenous mouse α-synuclein. The colon of 6-month-old mice from all three transgenic lines (Fig. 1B) revealed markedly increased amounts of protein that was approximately proportional to the greatly increased transcript levels seen by qPCR.

Motor function

By visual inspection the transgenic mice exhibited no gross motor dysfunction such as ataxia, tremor or paralysis. We examined motor function in the dbl-PAC-Tg($SNCA^{A53T}$)$^{+/+}$;$Snca^{-/-}$ and dbl-PAC-Tg($SNCA^{A30P}$)$^{+/+}$;$Snca^{-/-}$ mice against age-matched cohorts of PAC-Tg($SNCA^{WT}$)$^{+/+}$;$Snca^{-/-}$, wild-type $Snca^{+/+}$ and $Snca^{-/-}$ mice in two testing paradigms: accelerating Rotarod and open field. In the accelerating Rotarod test (Fig. 2), all three control lines, including the line overexpressing wild-type human *SNCA*, had similar latencies that decreased consistently, as expected, over four trials per day carried out over three consecutive days as the animals became more accustomed to and adept at staying on the rotating apparatus. We used 19–20 mice from each of the control lines at the 6 and 12 month time points and 10–12 control mice at the 18 month time point (Supplementary Material, Table S2). Both males and females of the dbl-PAC-Tg($SNCA^{A53T}$)$^{+/+}$;$Snca^{-/-}$ had consistent, significantly reduced latency beginning as early as 6 months. Abnormal latency persisted at 1 year of age and was even more striking for the dbl-PAC-Tg($SNCA^{A53T}$)$^{+/+}$;$Snca^{-/-}$ mice at the 18 month time point. We used 19–20 mice for these studies (Supplementary Material, Table S2).

In the open field apparatus, total distance travelled was similar in all three control lines, including the line overexpressing wild-type human *SNCA*. In contrast, total distance was significantly reduced in the dbl-PAC-Tg($SNCA^{A53T}$)$^{+/+}$;$Snca^{-/-}$ mice at 6 months and remained abnormal at 18 months of age, compared with controls (Fig. 3 and Supplementary Material, Table S3). With age, the dbl-PAC-Tg($SNCA^{A53T}$)$^{+/+}$;$Snca^{-/-}$ mice became even less active, travelling even less distance than did the control mice at 12 and 18 months. These studies used between 19 and 29 mice of each genotype (Supplementary Material, Table S3). The reduction in distance travelled was not specific to any particular type of movement or region in the open field such as center entries, differences in rearing behavior or less peripheral exploration. These results indicate there was a generalized reduction in movement that was not likely due to changes in exploratory behavior caused by anxiety. The body weight of mice expressing the A53T *SNCA* transgene was not significantly different from that of the control mouse strains measured out to 18 months of age (Supplementary Material, Fig. S1). The motor abnormalities seen in dbl-PAC-Tg($SNCA^{A53T}$)$^{+/+}$;$Snca^{-/-}$ mice therefore cannot be explained by their being heavier and less able to move.

In contrast, the dbl-PAC-Tg($SNCA^{A30P}$)$^{+/+}$;$Snca^{-/-}$ mice showed no motor abnormalities. The dbl-PAC-Tg($SNCA^{A30P}$)$^{+/+}$;$Snca^{-/-}$ had Rotarod latencies similar to controls at 6 or 12 months (Supplementary Material, Fig. S2) and no differences in total distance travelled in open field at either 6 or 12 months of age (Fig. 3). Analysis of male and female mice separately revealed no gender-specific differences in motor activity in dbl-PAC-Tg($SNCA^{A30P}$)$^{+/+}$;$Snca^{-/-}$ mice. These studies were performed on 29 and 24 PAC-Tg($SNCA^{A30P}$)$^{+/+}$;$Snca^{-/-}$ mice at 6 and 12 months, respectively, a large enough number that we should have seen any evident abnormalities (Supplementary Material, Table S3). We conclude that the PAC-Tg($SNCA^{A30P}$)$^{+/+}$;$Snca^{-/-}$ mice do not have the same degree of CNS dysfunction seen in the dbl-PAC-Tg($SNCA^{A53T}$)$^{+/+}$;$Snca^{-/-}$ mice.

In summary, dbl-PAC-Tg($SNCA^{A53T}$)$^{+/+}$;$Snca^{-/-}$ mice, but not dbl-PAC-Tg($SNCA^{A30P}$)$^{+/+}$;$Snca^{-/-}$ mice, demonstrated consistently reduced motor activity in the open field apparatus and abnormal endurance and coordination on the Rotarod compared with all three controls. It is interesting to note that included among the controls was the PAC-Tg($SNCA^{WT}$)$^{+/+}$;$Snca^{-/-}$ line, which overexpresses wild-type α-synuclein in brain at levels at least as great if not greater than what was seen with the $SNCA^{A53T}$ transgene.

Histological characterization of α-synuclein CNS pathology

Expression of α-synuclein in the brain and spinal cord of dbl-PAC-Tg($SNCA^{A53T}$)$^{+/+}$;$Snca^{-/-}$ mice was analyzed at 12 and 22 months of age to determine if these mice have the characteristic pathology of α-synuclein aggregates. Immunocytochemical analyses revealed a few rare dystrophic synapses in the hippocampus of 12- and 22-month-old dbl-PAC-Tg($SNCA^{A53T}$)$^{+/+}$;$Snca^{-/-}$ mice not found in control mice (Supplementary Material, Fig. S3a) but did not reveal widespread Lewy body pathology or α-synuclein aggregation. More specifically, the dorsal motor nucleus of the vagus, reported to be one of the first structures of the CNS affected by Lewy body and Lewy neurite pathology in idiopathic PD (2,4,36), showed no abnormalities of α-synuclein aggregation. The absence of widespread aggregates was confirmed by western blotting. High molecular weight, insoluble

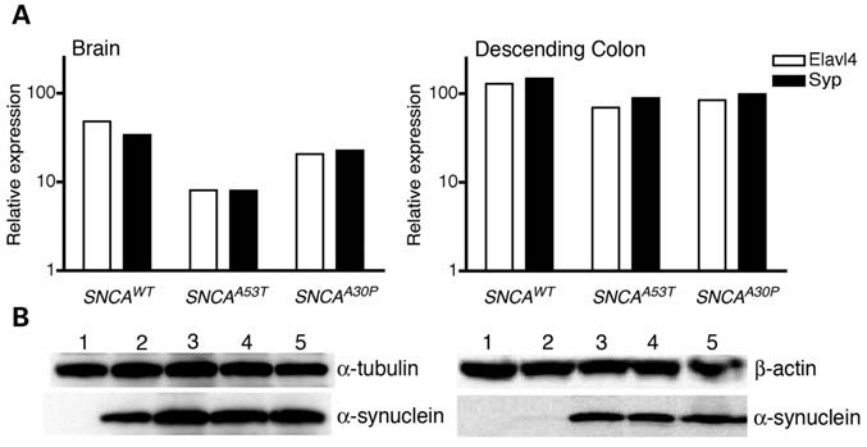

Figure 1. Transcript and protein expression in brain and distal colon. (**A**) qPCR measurements in 6-week-old mice of human *SNCA* transcript relative to endogenous mouse *Snca*, using the housekeeping genes *Elavl4* or synaptophysin as reference. Abbreviations are: $SNCA^{WT}$ is PAC-Tg($SNCA^{WT}$)$^{+/+}$;$Snca^{-/-}$, $SNCA^{A53T}$ is Dbl-PAC-Tg($SNCA^{A53T}$)$^{+/+}$;$Snca^{-/-}$ and $SNCA^{A30P}$ is Dbl-PAC-Tg($SNCA^{A30P}$)$^{+/+}$;$Snca^{-/-}$, Elav is *Elavl4, Syp* is synpatophysin. Transcript levels relative to endogenous *Snca* are shown on a logarithmic scale. Each data point represents the average of four replicates per sample averaged over 10 mice of the same genotype. qPCR data and calculations are in Supplementary Material, Table S1A and B. (**B**) Western blot of α-synuclein protein in 6-month-old mice with either endogenous α-tubulin (brain) or β-actin (colon) as loading controls. Lane 1, $Snca^{-/-}$; Lane 2, $Snca^{+/+}$; Lane 3, PAC-Tg($SNCA^{WT}$)$^{+/+}$; $Snca^{-/-}$; Lane 4, Dbl-PAC-Tg($SNCA^{A53T}$)$^{+/+}$;$Snca^{-/-}$; Lane 5, Dbl-PAC-Tg($SNCA^{A30P}$)$^{+/+}$;$Snca^{-/-}$.

aggregates of α-synuclein were absent in western blot analysis of brains from 6- to 18-month-old mice (Supplementary Material, Fig. S3b).

Dopamine and metabolite measurements

Striatal tissue DA and DA metabolite content were measured in 11- and 18-month-old controls and dbl-PAC-Tg($SNCA^{A53T}$)$^{+/+}$; $Snca^{-/-}$ mice by high performance liquid chromatography. Measurement at 11 months (data not shown) and 18 months (Supplementary Material, Fig. S4) revealed that total striatal dopamine, norepinephrine, the catecholaminergic metabolites 3,4-dihydroxyphenylacetic acid and homovanillic acid, serotonin (5-hydroxytryptamine) or the serotonin metabolite 5-hydroxyindoleacetic acid were not significantly different in dbl-PAC-Tg($SNCA^{A53T}$)$^{+/+}$;$Snca^{-/-}$ and control mice.

Stereology

To determine whether the motor abnormalities in the dbl-PAC-Tg($SNCA^{A53T}$)$^{+/+}$;$Snca^{-/-}$ mice were due to neurodegeneration, we performed unbiased stereological counting of both the tyrosine hydroxylase (TH)-immunoreactive neurons and the total neurons in SNpc at 11 and 18 months of age in age- and gender-matched transgenic and control mice (Supplementary Material, Fig. S5). Since the overexpressed $SNCA^{WT}$ or $SNCA^{A53T}$ transgenes were on a $Snca^{-/-}$ background, we were interested in determining whether (i) the $Snca^{-/-}$ background alone had fewer TH-immunoreactive neurons than the mouse $Snca^{+/+}$ wild-type at 11 or 18 months, (ii) the overexpressed $SNCA^{WT}$ or $SNCA^{A53T}$ transgenes on a $Snca^{-/-}$ background resulted in reduced TH-immunoreactive neurons compared with the $Snca^{-/-}$ background alone at 11 or 18 months and (iii) whether mice carrying overexpressed $SNCA^{WT}$ or $SNCA^{A53T}$ transgenes showed a loss of neurons between 11 and 18 months. None of these comparisons reached significance at the $P < 0.05$ level (with Bonferroni correction for multiple comparisons) except that the $Snca^{+/+}$ mice tended to have significantly more TH-immunoreactive neurons than did mice with any of the other three genotypes, but without any sign of progression. We conclude that there is no evidence for a progressive loss of dopaminergic SNpc neurons in dbl-PAC-Tg($SNCA^{A53T}$)$^{+/+}$;$Snca^{-/-}$ mice. In addition, the comparable numbers of neurons at 11 months in the $Snca^{-/-}$ mice versus mice overexpressing the $SNCA^{WT}$ or $SNCA^{A53T}$ transgenes on an $Snca^{-/-}$ background makes it unlikely that mice expressing the human transgenes have a deficit in neuronal development or survival.

ENS function

An early sign that colonic motility might be abnormal in the transgenic mice expressing mutant forms of *SNCA* was that the fecal pellets passed by mutant 6-month-old transgenic mice were abnormally small and hard. Timed collections of stool were carried out in cohorts of transgenic and control mice at various ages and the total stool weight and water content were measured. The total amount of stool passed/unit time and the stool water content were unchanged in the dbl-PAC-Tg($SNCA^{A53T}$)$^{+/+}$;$Snca^{-/-}$ animals at 3 months of age but by 6 months of age, each was significantly reduced to a comparable degree in both the dbl-PAC-Tg($SNCA^{A53T}$)$^{+/+}$; $Snca^{-/-}$ and dbl-PAC-Tg($SNCA^{A30P}$)$^{+/+}$;$Snca^{-/-}$ compared with controls (Fig. 4 and Supplementary Material, Table S4). The change in stool production and water content was even more marked by the time the dbl-PAC-Tg($SNCA^{A53T}$)$^{+/+}$; $Snca^{-/-}$ and dbl-PAC-Tg($SNCA^{A30P}$)$^{+/+}$;$Snca^{-/-}$ mice reached 12 months of age. The reduction in the wet weight of stool was due, not only to a reduction in water content, but also to a reduction in the dry mass of stool output.

Because a decrease in the propulsive motility of the colon would reduce both the amount of feces produced over a given period of time as well as its water content (37,38), we

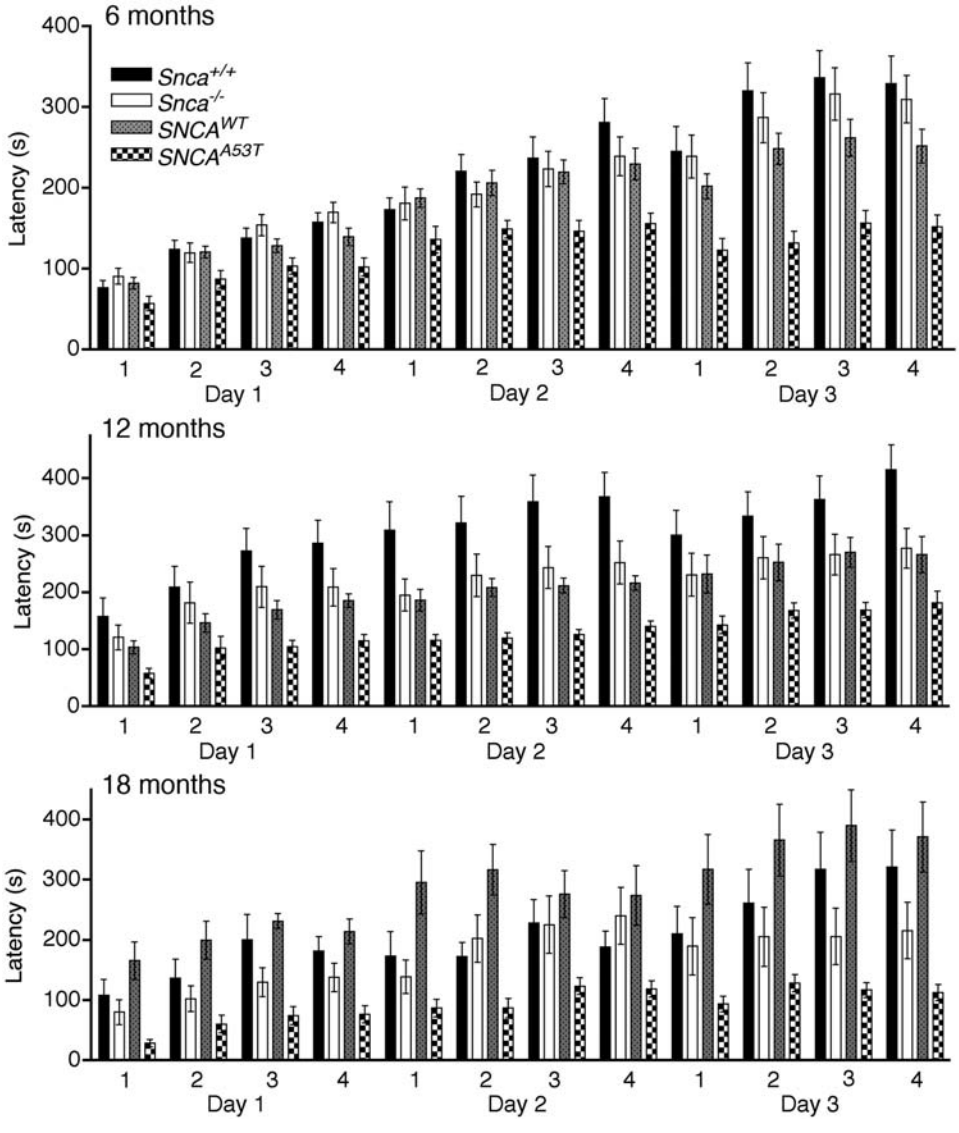

Figure 2. Latency (time to fall) in the Rotarod test at 6, 12 and 18 months of age. The pattern code corresponding to the various genotypes is given in the legend. Abbreviations are: $SNCA^{WT}$ is PAC-Tg($SNCA^{WT}$)$^{+/+}$;$Snca^{-/-}$ and $SNCA^{A53T}$ is Dbl-PAC-Tg($SNCA^{A53T}$)$^{+/+}$;$Snca^{-/-}$. Error bars are ± 1 standard errors of the mean. The number of mice of each genotype tested at each age is given in Supplementary Material, Table S2.

assessed the motility of the distal colon by measuring the time required to expel a bead inserted into the colon a distance of 2 cm above the anal verge (39). We found that the expulsion time was normally longer in male than in female mice in all of the animals tested, which is consistent with differences seen in anorectal manometry measurements in humans (40). This gender difference, however, was greatly exaggerated in male dbl-PAC-Tg($SNCA^{A53T}$)$^{+/+}$;$Snca^{-/-}$ mice, which required 4–5-fold more time than control mice to expel a bead. The prolongation in expulsion time appeared as early as 3 months of age and persisted through 18 months of age (Fig. 5 and Supplementary Material, Table S5). Female dbl-PAC-Tg($SNCA^{A53T}$)$^{+/+}$;$Snca^{-/-}$ mice also had prolonged expulsion times when compared with control female mice. A similar phenotype was seen in the males, but not the females, in dbl-PAC-Tg($SNCA^{A30P}$)$^{+/+}$;$Snca^{-/-}$ mice at 6 and 12 months, which were the oldest time points available for these mice. Interestingly, the dbl-PAC-Tg($SNCA^{WT}$)$^{+/+}$;$Snca^{-/-}$ mice showed no differences in colonic function compared with the $Snca^{+/+}$ or $Snca^{-/-}$ control mice despite massive overexpression of the protein in the colon.

We next examined whole-gut transit time (WGTT). As early as 3 months of age, dbl-PAC-Tg($SNCA^{A53T}$)$^{+/+}$;$Snca^{-/-}$ mice demonstrated significantly prolonged WGTT compared with $Snca^{+/+}$ ($P = 0.026$) or $Snca^{-/-}$ ($P = 0.0055$) control mice (Mann–Whitney test; Fig. 6 and Supplementary Material, Table S6). WGTT was also prolonged compared with the PAC-Tg($SNCA^{WT}$)$^{+/+}$;$Snca^{-/-}$ control but did not quite reach significance ($P = 0.075$). By 6 months of age, dbl-PAC-Tg($SNCA^{A53T}$)$^{+/+}$;$Snca^{-/-}$ showed markedly prolonged WGTT compared with each of the three control lines, and the prolongation persisted through 18 months of age.

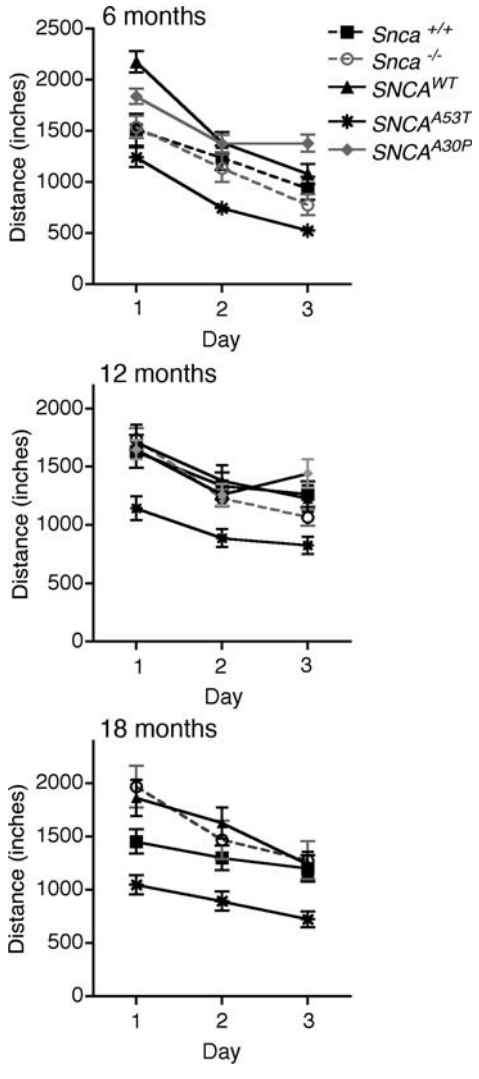

Figure 3. Total distance travelled in open field at 6, 12 and 18 months of age. Symbols distinguishing the line graphs for the different genotypes are in the legend. There are no data at the 18 month time point for the Dbl-PAC-Tg($SNCA^{A30P}$)$^{+/+}$;$Snca^{-/-}$ line. Abbreviations are: $SNCA^{WT}$ is PAC-Tg($SNCA^{WT}$)$^{+/+}$;$Snca^{-/-}$, $SNCA^{A53T}$ is Dbl-PAC-Tg($SNCA^{A53T}$)$^{+/+}$; $Snca^{-/-}$ and $SNCA^{A30P}$ is Dbl-PAC-Tg($SNCA^{A30P}$)$^{+/+}$;$Snca^{-/-}$. Error bars are ± 1 standard errors of the mean. The number of mice of each genotype tested at each age is given in Supplementary Material, Table S3.

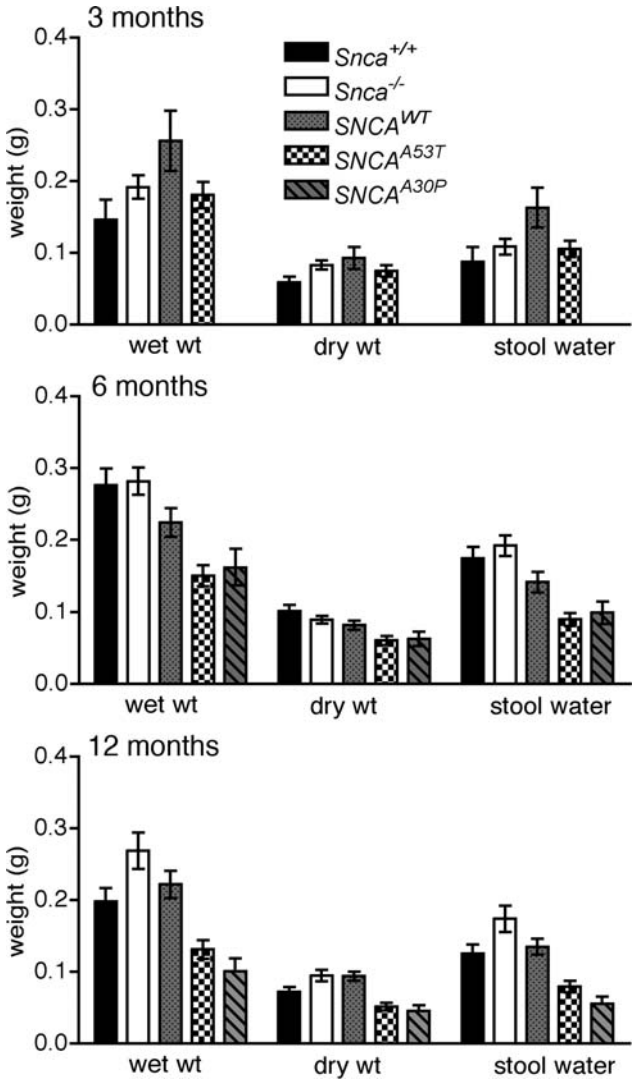

Figure 4. Total and dry stool weight and the difference (water content) collected over 1 h from 10 to 11 AM. The pattern code corresponding to the various genotypes is given in the legend. Abbreviations are: $SNCA^{WT}$ is PAC-Tg($SNCA^{WT}$)$^{+/+}$;$Snca^{-/-}$, $SNCA^{A53T}$ is Dbl-PAC-Tg($SNCA^{A53T}$)$^{+/+}$; $Snca^{-/-}$ and $SNCA^{A30P}$ is Dbl-PAC-Tg($SNCA^{A30P}$)$^{+/+}$;$Snca^{-/-}$. Error bars are ± 1 standard errors of the mean. The number of mice of each genotype tested at each age is given in Supplementary Material, Table S4. There are no data for $SNCA^{A30P}$ at 3 months.

A similar significant prolongation of WGTT was seen in dbl-PAC-Tg($SNCA^{A30P}$)$^{+/+}$;$Snca^{-/-}$ mice at 3 months of age. By 6 months and again at 12 months of age, dbl-PAC-Tg($SNCA^{A30P}$)$^{+/+}$;$Snca^{-/-}$ mice continued to show prolonged WGTT. In contrast to the bead expulsion time, the marked prolongation in transit time did not differ between males and females. Interestingly, the PAC-Tg($SNCA^{WT}$)$^{+/+}$; $Snca^{-/-}$ line again did not differ significantly from the $Snca^{+/+}$ or $Snca^{-/-}$ control mice in WGTT.

We conclude that the comparably prolonged WGTT and reduced colonic motility in both double-PAC transgenic lines indicate that the dysfunction in these mice is not an idiosyncratic effect of particular transgenic insertions but, instead, is intrinsic to the presence of a mutant, and not wild-type, human α-synuclein expressed from the human genomic sequence in the PAC transgenes. These results are in contrast with the motor changes, which were more subtle and restricted to the A53T transgenic line. This constellation of phenotypic findings is particularly interesting given the early ENS dysfunction seen in PD patients prior to the development of their parkinsonian motor dysfunction.

Histological characterization of α-synuclein ENS pathology

Immunofluorescence of whole-mount preparations, double-labeled with antibodies against α-synuclein and the neuronal marker HuC/D, showed that the overexpressed α-synuclein in

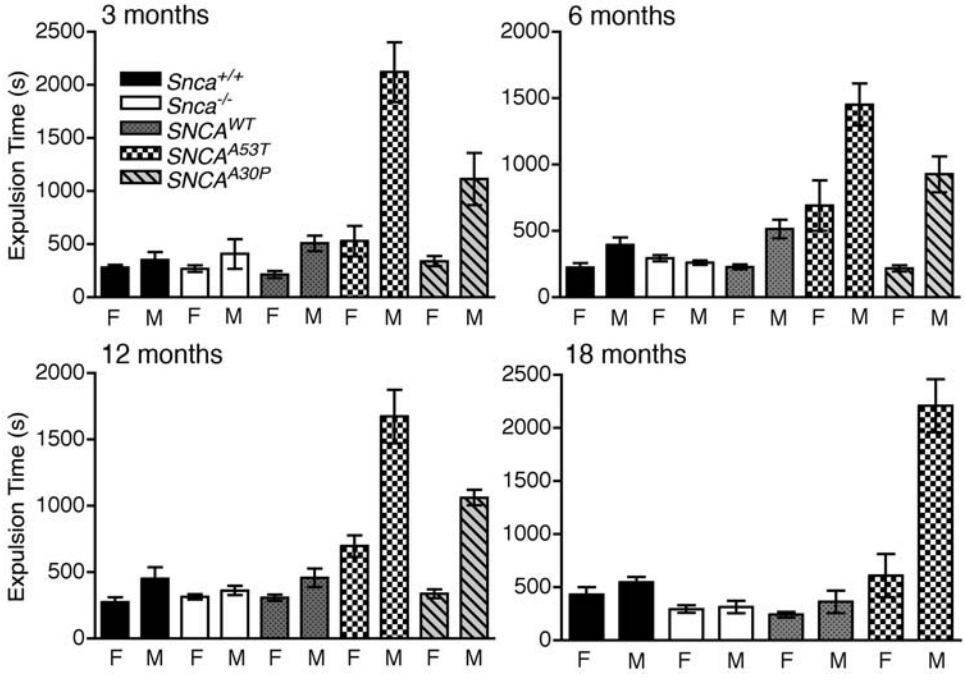

Figure 5. Colonic motility at 3, 6, 12 and 18 months as assessed by time in seconds required for a bead to be expelled from the rectum, plotted separately for males and females. The pattern code corresponding to the various genotypes is given in the legend. Abbreviations are: $SNCA^{WT}$ is PAC-Tg($SNCA^{WT}$)$^{+/+}$; $Snca^{-/-}$, $SNCA^{A53T}$ is Dbl-PAC-Tg($SNCA^{A53T}$)$^{+/+}$;$Snca^{-/-}$ and $SNCA^{A30P}$ is Dbl-PAC-Tg($SNCA^{A30P}$)$^{+/+}$;$Snca^{-/-}$. There are no data at the 18 month time point for the Dbl-PAC-Tg($SNCA^{A30P}$)$^{+/+}$;$Snca^{-/-}$. Error bars are ± 1 standard errors of the mean. The number of mice of each genotype tested at each age is given in Supplementary Material, Table S5.

the dbl-PAC-Tg($SNCA^{A53T}$)$^{+/+}$;$Snca^{-/-}$ line was present in TH-immunoreactive neuronal cell bodies within both myenteric and submucosal plexuses, but not in the varicose TH positive terminals of noradrenergic sympathetic neurons (Fig. 7). Most of the α-synuclein-immunoreactive neurons, particularly in the myenteric plexus, however, were not coincident with TH immunoreactivity. Lewy bodies in human patients have been reported to be present in neurons containing both vasoactive intestinal peptide (VIP) and nitric oxide synthase (NOS); therefore, we determined whether the non-dopaminergic α-synuclein-immunoreactive neurons were NOS-immunoreactive. Double label immunocytochemistry was carried out to locate α-synuclein and NOS. Surprisingly, the immunoreactivity for α-synuclein was largely excluded from NOS-immunoreactive neurons (Fig. 8) in both the myenteric and submucosal plexuses of the small and large intestines. Some NOS-immunoreactive neurons, however, were surrounded by α-synuclein-immunoreactive varicose axon terminals, suggesting that these neurons are innervated by α-synuclein-containing synapses. As expected, the α-synuclein was concentrated in synapses, as demonstrated by coincident localization with the synaptic protein synaptotagmin (Fig. 9). Not all synaptotagmin-immunoreactive synapses contained α-synuclein and some -synuclein-immunoreactive varicosities lacked synaptotagmin and thus were not synapses. We also observed areas within neuronal cell bodies showing immunoreactivity with α-synuclein but not synaptotagmin. To investigate these further, we determined whether these aggregates could be immunostained with antibodies to -α-synuclein following digestion of tissue with proteinase K. This analysis revealed numerous proteinase K-resistant α-synuclein aggregates in the nuclear and perinuclear cytoplasm of ENS neurons in the dbl-PAC-Tg($SNCA^{A53T}$)$^{+/+}$;$Snca^{-/-}$ mice that showed gastrointestinal motility dysfunction but not in the PAC-Tg($SNCA^{WT}$)$^{+/+}$;$Snca^{-/-}$ that lacked the signs of ENS dysfunction (Fig. 10).

Olfaction

Besides the motor symptoms of parkinsonism and ENS dysfunction, patients with PD have a high incidence of hyposmia and autonomic instability (5). Hyposmia is a common early symptom in PD, often occurring prior to the onset of the movement abnormality and independent of medical therapy (41). We tested olfaction in dbl-PAC-Tg($SNCA^{A53T}$)$^{+/+}$;$Snca^{-/-}$ mice with two different tests of olfaction: time spent exploring a novel odor and latency to locate food buried beneath the bedding. In both tests PAC transgenic and control mice performed similarly (Supplementary Material, Fig. S6). No olfactory deficit was seen in the dbl-PAC-Tg($SNCA^{A30P}$)$^{+/+}$;$Snca^{-/-}$ mice as well. In addition, histological examination of the olfactory bulbs from PAC transgenic mice showed no neurodegeneration or protein aggregation (data not shown). Thus, in this model, the ENS is affected well before the olfactory neurons show any pathological or functional abnormality.

Autonomic cardiac innervation

Dysfunction of diurnal autonomic cardiovascular regulation, manifest as cardiac sympathetic denervation and reduced

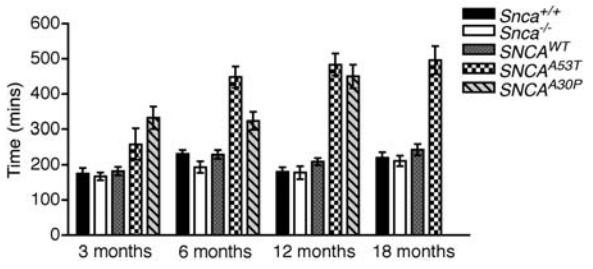

Figure 6. Whole-gut transit time at 3, 6, 12 and 18 months as determined by time in minutes required for a non-absorbable dye introduced by gavage to appear in the stool. The pattern code corresponding to the various genotypes is given in the legend. Abbreviations are: $SNCA^{WT}$ is PAC-Tg$(SNCA^{WT})^{+/+}$; $Snca^{-/-}$, $SNCA^{A53T}$ is Dbl-PAC-Tg$(SNCA^{A53T})^{+/+}$;$Snca^{-/-}$ and $SNCA^{A30P}$ is Dbl-PAC-Tg$(SNCA^{A30P})^{+/+}$;$Snca^{-/-}$.There are no data at the 18 month time point for the Dbl-PAC-Tg$(SNCA^{A30P})^{+/+}$;$Snca^{-/-}$. Error bars are ± 1 standard errors of the mean. The number of mice of each genotype tested at each age is given in Supplementary Material, Table S6.

heart rate variability, have been described both in sporadic PD (42) and in a family with autosomal dominant PD due to triplication of the α-synuclein gene (43). We carried out 24 h Holter monitor recordings by telemetry in 12-month-old dbl-PAC-Tg$(SNCA^{A53T})^{+/+}$;$Snca^{-/-}$ versus $Snca^{-/-}$ control mice. We examined heart rate variability and performed both time-domain and frequency-domain spectral analysis of heart rate to assess the mice for autonomic dysfunction (44). The power of the low- and high-frequency components were the same in the transgenic and $Snca^{-/-}$ mice. The ratio of low-frequency to high-frequency spectral components, a measure of sympathovagal balance, was unchanged as was the standard deviation of beat-to-beat variation (Supplementary Material, Fig. S7). These data indicate there were no significant dysfunction of the autonomic nervous system as reflected in the autonomic regulation of heart rate in the transgenic mice versus $Snca^{-/-}$ controls as of 12 months of age.

DISCUSSION

We have documented profound, early ENS dysfunction in two transgenic lines of mice carrying insertions of a human PAC containing the entire human *SNCA* gene. The PAC was engineered to contain either the A53T or the A30P mutation previously shown to cause autosomal dominant PD in families and the mice were crossed to mice with a knock-out mutation in the endogenous *Snca* gene so that the only α-synuclein in these mice was a human mutant protein. An artificial chromosome was chosen for expressing α-synuclein in these models because it contained the entire human *SNCA* gene with its normal exon and intron structure as well as 35 kb of upstream sequences. Although the regulatory elements controlling *SNCA* expression have not been completely defined, there are clearly upstream promoter elements as well as regulatory sequences in the first intron (45,46). Thus, expression in these transgenic mice would likely be driven and controlled by endogenous gene regulatory elements. We found that transcript and protein expression were both markedly increased in the ENS of the colon in these mice over what was seen in endogenous mouse GI tract. The ENS dysfunction was reflected in reduced total fecal mass and fecal water content per unit time, increased time required to expel a bead from the colon, and increased WGTT in both lines carrying the PD-associated mutations, A53T and A30P, but not from an equally overexpressed wild-type *SNCA* transgene. Given that these lines were independently generated and expressed different PD-associated mutations, the ENS dysfunction must be the direct result of overexpression of the mutant α-synucleins and not a non-specific effect of differences in genetic background, position effects from the transgene insertions or mutations at insertion sites.

ENS dysfunction could already be seen as early as 3 months of age, reached its maximum severity by 6 months of age and then persisted to 18 months. The ENS dysfunction occurred at a young age, before there was any evidence of olfactory or dysfunction in the autonomic innervation of the heart and before there were pathological changes in the brain stem. The lack of autonomic dysfunction, as seen in 24-h heart rate variability measurements and the absence of pathological changes in the brain stem, including the dorsal motor nucleus of the vagus [one of the first structures of the CNS affected by Lewy body and Lewy neurite pathology in idiopathic PD (2,4,36)], suggest that the ENS dysfunction in the mice is an *intrinsic* defect caused by mutant α-synuclein expression and aggregation in the ENS rather than to an *extrinsic* effect of abnormal central innervation of the gut.

Wang *et al*. (47) previously reported colonic dysfunction in 12-month-old male transgenic mice in which wild-type α-synuclein expression was driven by the heterologous Thy-1 promoter (Thy1-αSynuclein). These mice exhibited decreased fecal output that increased to control levels in response to corticotropin releasing factor. However, they saw no significant change in colonic motility (measured by bead expulsion) and observed what seemed to be a trend towards increased fecal output of the Thy1-α-synuclein mice when they were placed in a novel environment. Our studies showed abnormalities only when the mutant human α-synuclein was expressed, and not the human protein, despite the fact that levels of transcript and protein expression in the mice with wild-type constructs were at least as great, if not greater. Finally, we observed that not only was colonic motility abnormal, but WGTT was also markedly prolonged. The effect on WGTT was seen regardless of the sex of the mouse and is indicative of widespread ENS abnormalities.

One interesting observation is that colonic propulsion in mice is strikingly different depending on gender. Gender differences in anorectal function have not been reported previously in mice but are quite consistent with observations made in humans. Human males have a greater sphincter length at rest and with squeezing, and the mean maximum squeeze pressure required for defecating are significantly greater in males than in females (40).

Increased gastrointestinal transit time, constipation and difficulty with defecation are common in the course of sporadic PD and occur well before the movement disorder appears (7–9,31). The gastrointestinal dysfunction is unlikely to be a secondary consequence of the movement disorder itself since patients with parkinsonism due to lacunar infarcts in the caudate, putamen or globus pallidus do not have the same gastrointestinal difficulties (8). The gastrointestinal dysfunction also does not result from the medications used to treat

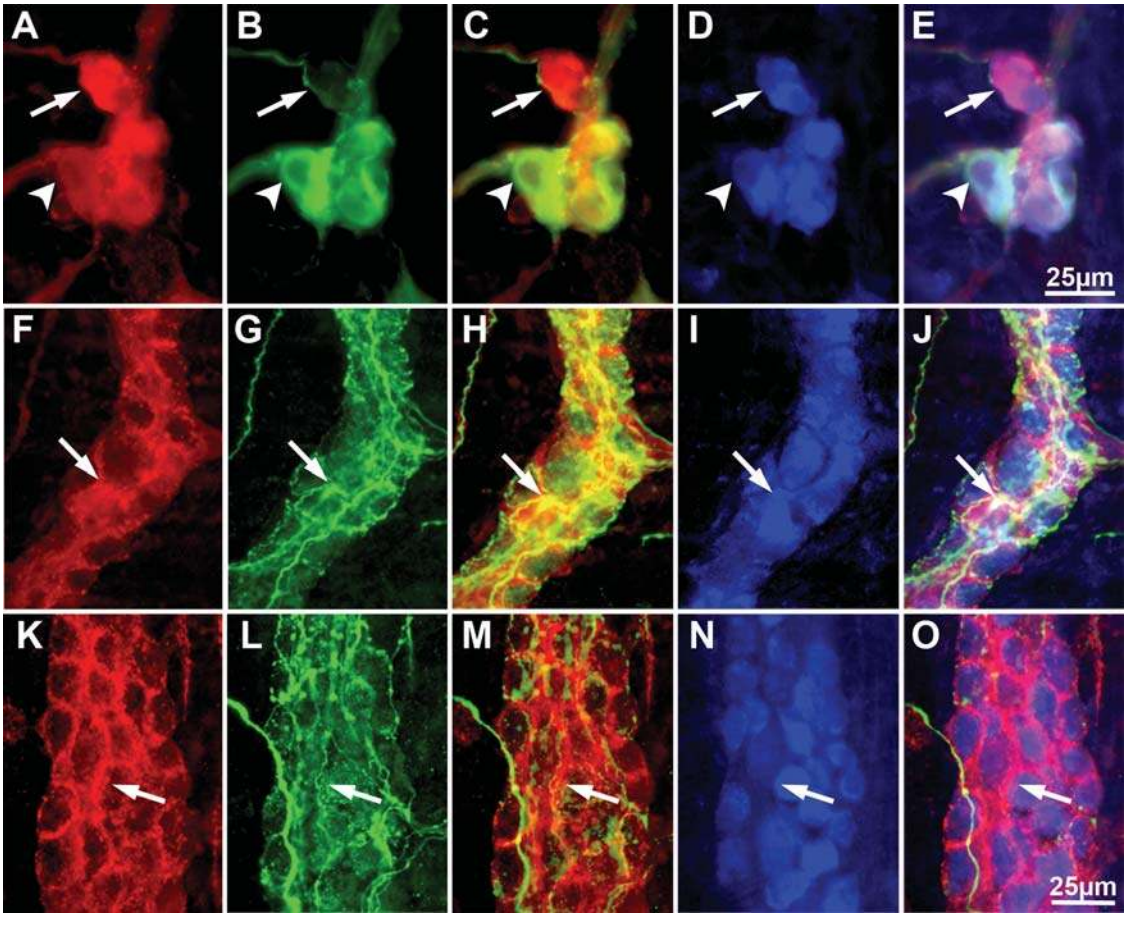

Figure 7. Coincident location of α-synuclein and TH immunoreactivities occur in enteric neurons of dbl-PAC (Tg*SNCA*^{A53T}); Snca$^{-/-}$ mice. α-synuclein immunoreactivity is illustrated in A, F and K. TH immunoreactivity is illustrated in B, G and L. Merged α-synuclein/TH immunoreactivities are shown in C, H and M. The immunoreactivity of the neuronal marker Hu is illustrated in D, I and N. The triple merge of all immunoreactivities is shown in E, J and O. (**A**–**E**) Submucosal ganglion in the ileum. Most, but not all (arrow) α-synuclein-immunoreactive neurons also contain TH immunoreactivity (arrowhead). Because all of the α-synuclein-immunoreactive cells are Hu-immunoreactive, they are neurons. (**F**–**J**) Myenteric ganglion in the ileum. Aggregates of α-synuclein immunoreactivity (F) are found in one TH-immunoreactive neuron. Note that most of the TH immunoreactivity in the mytenteric plexus is found in varicose sympathetic axons, which do not contain α-synuclein or Hu immunoreactivities. Axons lack Hu, which is confined to neuronal perikarya. (**K**–**O**) Myenteric ganglion of the distal colon. Most of the α-synuclein immunoreactivity is found in axons that lack TH immunoreactivity (arrow). The markers = 25 μm.

the movement disorder since gastrointestinal dysfunction is common in newly diagnosed PD patients prior to the initiation of drug treatment (48). Decreased bowel movement (BM) frequency in early adulthood is strongly associated with the development of Lewy body pathology indicative of PD later in life. In the longitudinal Honolulu Asia Aging Study, 245 men without PD were followed and later died and came to autopsy (11,49). Those with <1 or 1 BM/day had 4.3-fold and 2.2-fold increased odds, respectively, of incidental LB on autopsy compared than in those with >1 BM/day. A large body of evidence supports the conclusion that ENS dysfunction is an early, intrinsic component of the PD phenotype.

In light of the findings reported here, it would be interesting to know whether the familial form of PD due to α-synuclein mutations also starts in the ENS. Although detailed clinical descriptions of affected individuals from the families with the A53T or A30P mutations have been published (50,51), the authors of these studies only provide clinical data for motor and cognitive abnormalities and do not comment on the presence or absence of gastrointestinal dysfunction.

Braak and his co-workers have reported that many individuals without any signs of PD at the time of death have Lewy bodies in the ENS, as well as in the olfactory bulbs and the dorsal motor nucleus of the vagus, but not in the substantia nigra or other areas of the CNS typically affected in PD (2–4,14,36,52). The Lewy bodies in the ENS found at autopsy in individuals who lack the motor symptoms of PD are often in VIP-containing neurons of the myenteric and submucosal plexuses (16,17,53,54). Assuming that incidental Lewy body pathology in asymptomatic individuals represents the earliest stages of PD, Braak *et al*. proposed a staging scheme in which a presymptomatic phase, characterized by ENS, brainstem and olfactory bulb pathology, is succeeded by a symptomatic phase when the movement disorder becomes manifest, characterized by pathology in the midbrain, including substantia nigra and ending with a cortical phase, with widespread cortical Lewy bodies. Because of the limitations of autopsy studies, the scheme was not able to establish the temporal relationship between the enteric Lewy bodies and other early pathological changes in the olfactory bulb or brainstem. Although Braak's

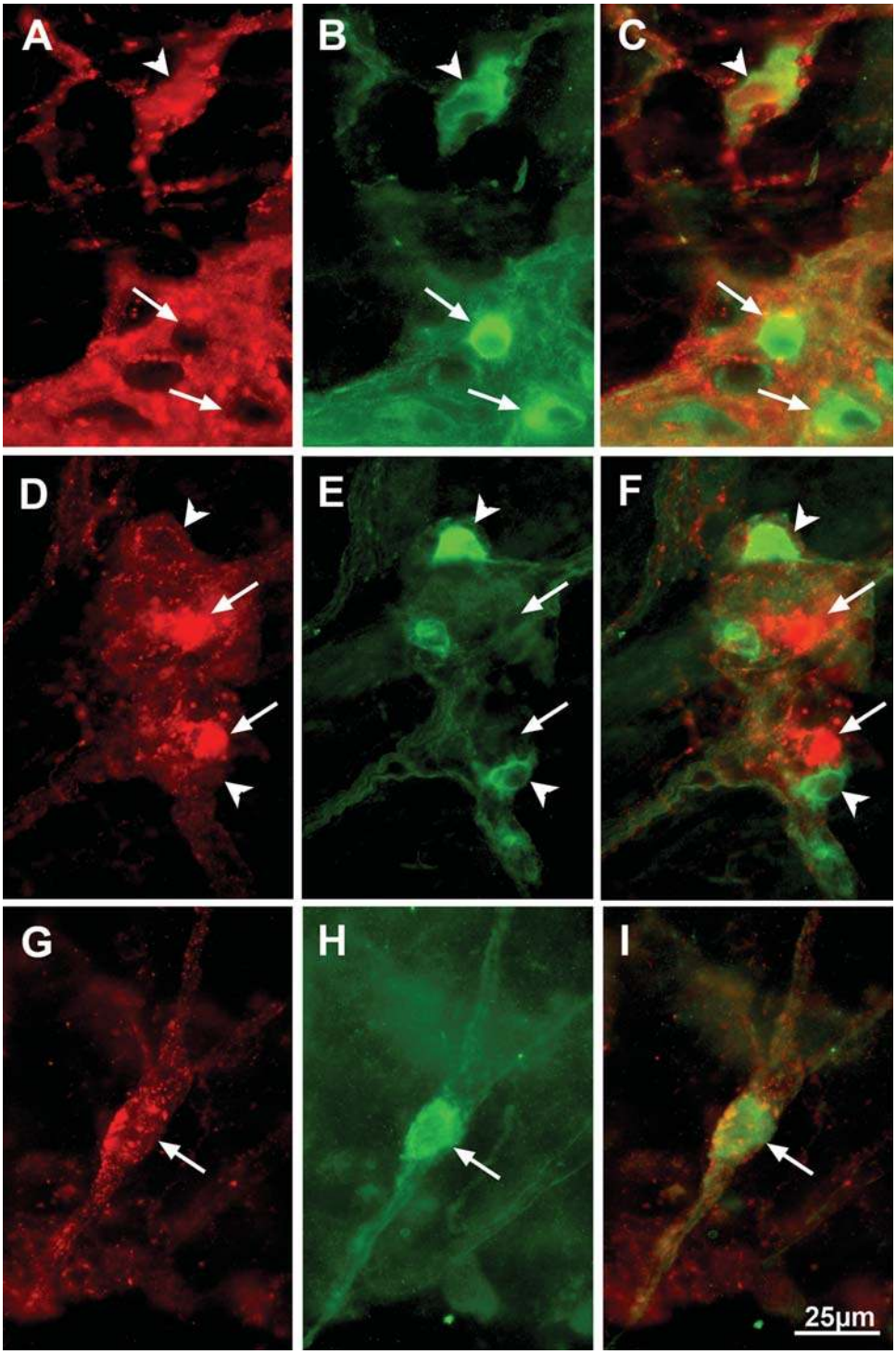

Figure 8. NOS-immunoreactive enteric neurons of dbl-PAC (Tg*SNCA*^{A53T}); *Snca*$^{-/-}$ mice do not display α-synuclein immunoreactivity. α-synuclein immunoreactivity is illustrated in A, D and G. NOS immunoreactivity is illustrated in B, E and H. Merged α-synuclein/NOS immunoreactivities are shown in C, F and I. (**A**–**C**) Gastric myenteric ganglion. Most NOS-immunoreactive neurons do not contain α-synuclein immunoreactivity (arrows); however, NOS and α-synuclein immunoreactivities are co-localized in a small number of neurons (arrowhead). (**D**–**F**) Ileal myenteric ganglion. α-synuclein immunoreactivity (arrows) and NOS immunoreactivity (arrowheads) are located in different neurons. (**G**–**I**) Submucosal ganglion of proximal colon. A neuron that expresses NOS immunoreactivity (H) is surrounded by α-synuclein-immunoreactive varicose axon terminals, suggesting that the NOS-immunoreactive neuron is innervated by α-synuclein-containing synapses (G). The markers = 25 μm.

staging schema has been criticized by some for being oversimplified and tainted with ascertainment bias (55,56), it has also received additional support (57). At a minimum, it has drawn the attention of researchers to the early, non-motor signs of the disease and away from an exclusive focus on dopaminergic neuronal loss and the parkinsonian movement disorder.

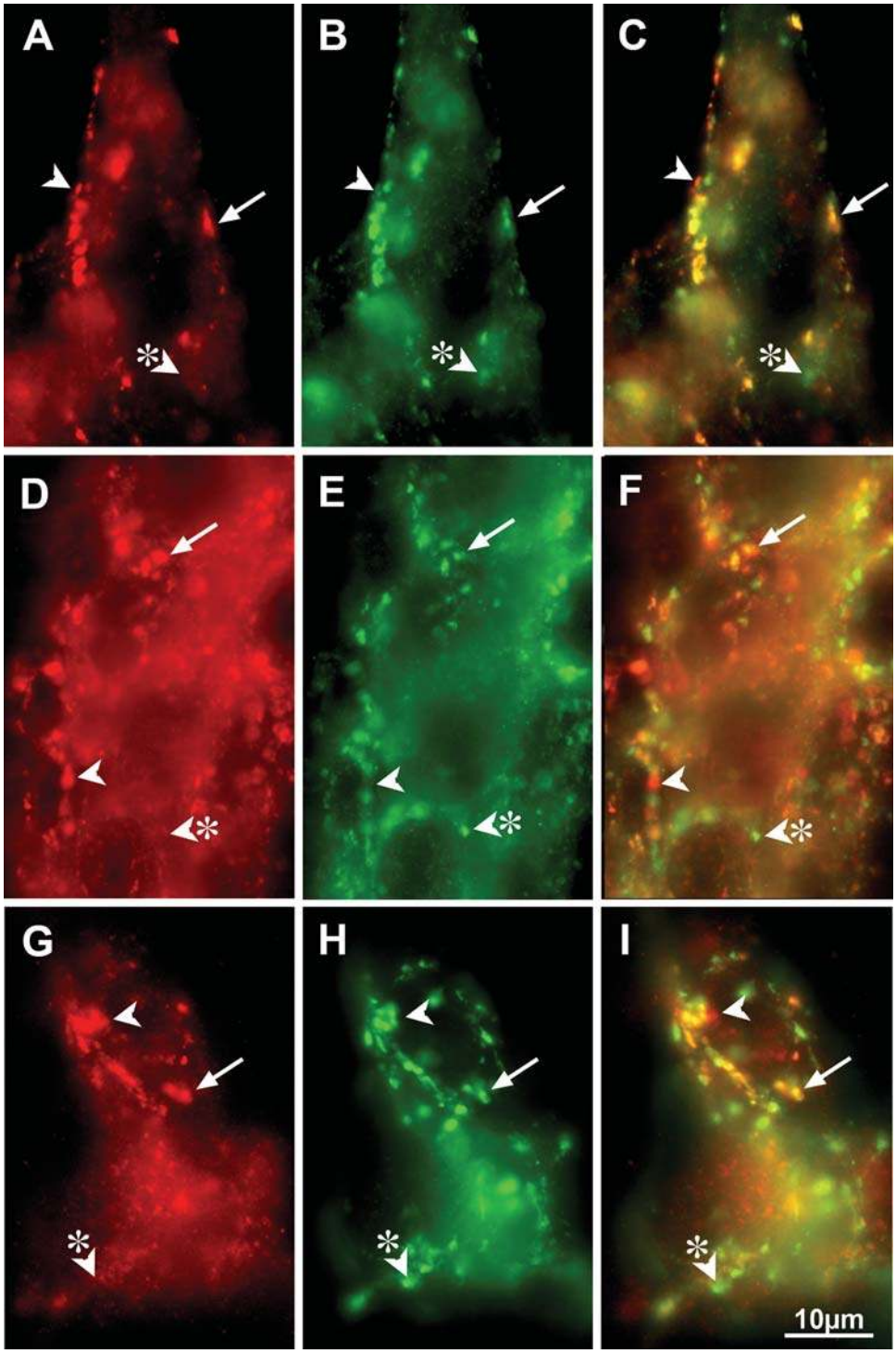

Figure 9. α-synuclein and synaptotagmin immunoreactivities are coincident in varicose terminal axons in the ENS of dbl-PAC (Tg*SNCA*^{A53T}); *Snca*$^{-/-}$ mice. α-synuclein immunoreactivity is illustrated in A, D and G. Synaptotagmin immunoreactivity is illustrated in B, E and H. Merged α-synuclein/synaptotagmin immunoreactivities are shown in C, F and I. (**A**–**C**) Myenteric ganglion of the stomach. Almost all α-synuclein immunoreactivity is colocalized with synaptotagmin immunoreactivity in axon terminal varicosities (arrows); nevertheless, a small number of apparent α-synuclein-immunoreactive varicosities lack synaptotagmin immunoreactivity (arrowhead) and thus are not synapses. Similarly, a small number of synaptotagmin-immunoreactive synapses (arrowhead with asterisk) lack α-synuclein. (**D**–**F**) An ileal myenteric ganglion. Most varicose axon terminals (arrows) contain coincident α-synuclein and synaptotagmin immunoreactivities; however, as in the stomach, small numbers of α-synuclein-immunoreactive varicose expansions lack synaptotagmin (arrowhead) and small numbers of synaptotagmin-immunoreactive synapses lack α-synuclein (arrowhead with asterisk). (**G**–**I**) Submucosal ganglion in the ileum. Again, α-synuclein and synaptotagmin immunoreactivities are extensively colocalized in varicose axon terminals (arrow). As in the stomach and ileum (arrowhead and arrowhead with asterisk), the coincident localization is incomplete. The markers = 10 μm.

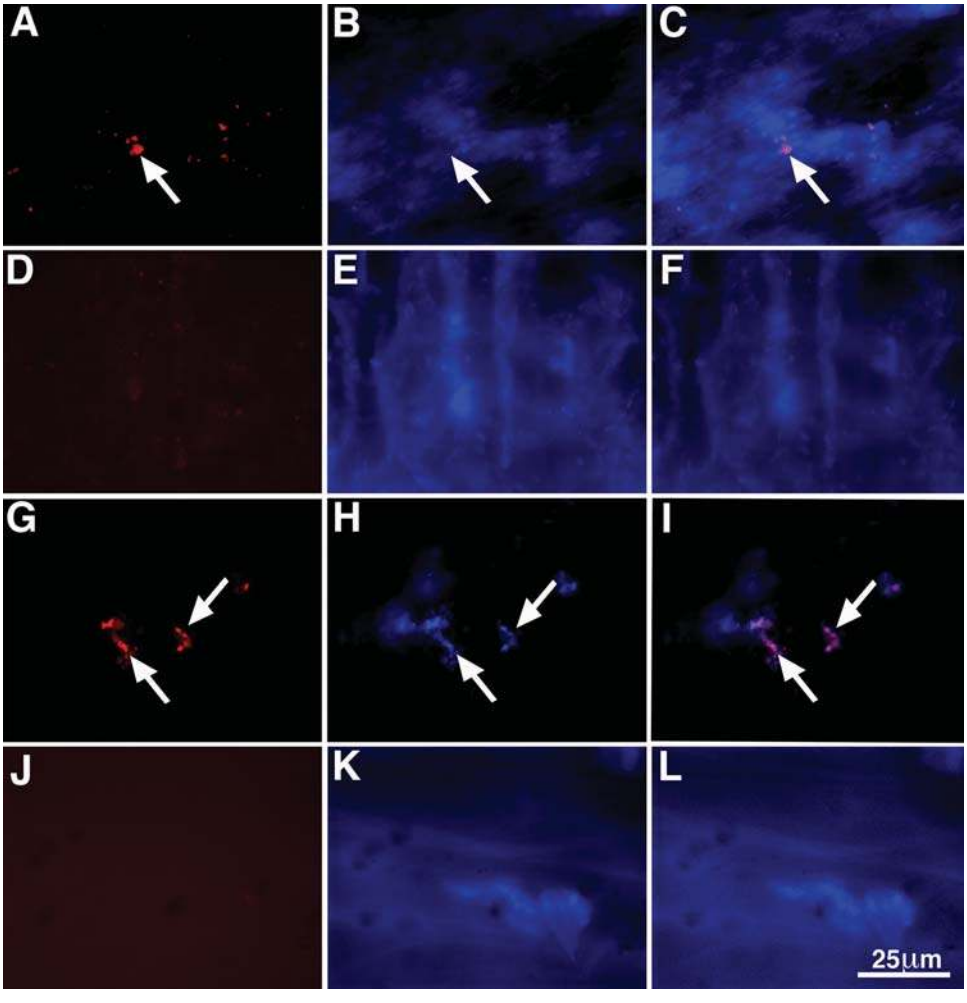

Figure 10. Aggregates of α-synuclein immunoreactivity that resist digestion with proteinase K are found in enteric neurons of Dbl-PAC-Tg($SNCA^{A53T}$); *Snca* −/− mice. (**A**–**C**) Myenteric plexus from the ileum of a Dbl-PAC-Tg($SNCA^{A53T}$); *Snca* −/− mouse. (A) Aggregates of α-synuclein immunoreactivity (arrow) are found in neurons of the myenteric plexus. (B) Bisbenzamide fluorescence of the field illustrated in A. There is some diffusion of bisbenzamide fluorescence due to the digestion of tissue with proteinase K; however, the locations of large neuronal nuclei are evident. (C) Merged image of Alexa 594 and bisbenzamide fluorescence. (**D**–**F**) Myenteric plexus from the ileum of a PAC-Tg($SNCA^{WT}$); *Snca* −/− mouse. (D) There is no remaining α-synuclein immunoreactivity after digestion of tissue with proteinase K. (E) Bisbenzamide fluorescence. (F) Merged image of Alexa 594 and bisbenzamide fluorescence. (**G**–**I**) Submucosal plexus from the ileum of a Dbl-PAC-Tg($SNCA^{A53T}$); *Snca* −/− mouse. (G) Aggregates of α-synuclein immunoreactivity (arrows) are found in neurons of the submucosal plexus. (H) Bisbenzamide fluorescence of the field illustrated in A. (I) Merged image of Alexa 594 and bisbenzamide fluorescence. (**J**–**L**) Submucosal plexus from the ileum of a PAC-Tg($SNCA^{WT}$); *Snca* −/− mouse. (J) There is no remaining α-synuclein immunoreactivity after proteinase K digestion of tissue. (K) Bisbenzamide fluorescence. (L) Merged image of Alexa 594 and bisbenzamide fluorescence. The marker = 25 μm.

There is ample evidence that the movement disorder seen in PD results from loss of dopaminergic neurons in the substantia nigra and other regions of the CNS (58). There also appears to be a role for dopaminergic dysfunction in ENS function in PD as well. Human PD patients with abnormal colonic motility reportedly show reduced ENS dopamine levels and a loss of dopaminergic neurons in the colon (53). Studies in rodents also indicate that dopaminergic neurons are important for colonic motility. Dopaminergic neurons are present as intrinsic components of both the submucosal and myenteric plexus of rodent ENS and changes in dopaminergic function are associated with marked changes in colonic motility (59,60). We saw overexpression of α-synuclein in dopaminergic neuronal cell bodies but not in the extrinsic sympathetic noradrenergic projections to the bowel. It seems unlikely, however, that the ENS dysfunction in the mutant α-synuclein transgenic mice is due entirely to a defect in dopaminergic function since the overexpressed protein was also seen in other types of neuron. Mice treated acutely with MPTP (1-methyl 4-phenyl 1,2,3,6-tetrahydropyridine) had a 40% reduction in colonic dopaminergic neurons but only a transiently abnormal colonic motility and no gastric or small intestine motility deficits (61). In the small intestine of normal rats, only a small fraction of neurons are α-synuclein-immunoreactive and, depending on which part of the stomach or small intestine is being studied, the expression is predominantly coincident with nitrergic and cholinergic, but not TH-immunoreactive, neurons (62). Thus, it is likely that a number of different neurotransmitter-defined neurons, in addition to those that contain dopamine are impaired to cause the ENS dysfunction reported here. Careful studies with dopamine and other neurotransmitter

agonists and antagonists may help to determine which neurons are most responsible for the mutant α-synuclein-induced motor abnormalities of the bowel.

Along with robust signs of ENS dysfunction, the dbl-PAC-Tg($SNCA^{A53T}$)$^{+/+}$;$Snca^{-/-}$ mice, also exhibited reproducible abnormalities in motor function detected by rotarod and open field measurements as early as 6 months of age. The movement abnormalities occurred in the absence of changes typical of PD in the CNS such as Lewy body pathology, neurodegeneration or even changes in striatal dopamine levels. As reviewed by Chesselet (27), Meredith *et al*. (28), Terzioglu and Galter (29) and Melrose *et al*. (30), most transgenic rodent models have little or no CNS pathology and none fully recapitulate PD, although, in some cases, rare protein aggregates with Lewy-body-like pathology occur. In a few transgenic models, massive non-physiological overexpression of α-synuclein in cells, such as the motor neurons of the anterior horn of the spinal cord, which usually express only low levels of α-synuclein in comparison to other parts of the CNS, results in lower motor neuron degeneration that is not characteristic of human PD (33,63). We conclude that even modest overexpression of the mutant A53T α-synuclein can subtly interfere with normal neuronal function in both the CNS and ENS prior to the development of frank neurodegeneration. Motor dysfunction was, however, not seen in the dbl-PAC-Tg($SNCA^{A30P}$)$^{+/+}$;$Snca^{-/-}$ despite expression levels of transcript and protein equivalent to the dbl-PAC-Tg($SNCA^{A53T}$)$^{+/+}$;$Snca^{-/-}$ mice. Why mice overexpressing A53T and not A30P α-synuclein showed abnormalities on rotarod and open field testing is not known. One possibility is that the A30P mutation may be a less severe mutation than the A53T mutation. For example, the average age of onset of the motor abnormalities of PD was 45.6 ± 13.5 years in the large Italian–American kindred with the A53T mutation described by Duvoisin, Golbe and their colleagues and 59.7 ± 10.8 years in the German family with the A30P mutation reported by Krüger *et al*. (50,51). This difference just reaches statistical significance ($P = 0.04$, two-tailed *t*-test).

Compared with the ENS, α-synuclein protein expression in the brain was only modestly increased despite very substantial increases in transcript levels. These findings suggest there are mechanisms by which the brain can regulate α-synuclein levels despite increased steady-state human *SNCA* transcript. Such regulation could be at the level of protein translation or degradation and remains to be elucidated.

Our results support the view that, just as has been suggested for sporadic PD, familial PD due to abnormalities in α-synuclein, manifests early, perhaps even first, in the ENS. The early onset of robust ENS dysfunction in the PAC transgenic mice described here is a convenient mammalian model system with simple assays in which to study interventions designed to reverse the deleterious effects of α-synuclein overexpression. They also could be viewed as a sensitized model in which to investigate the role of additional factors in the pathogenesis of PD. Braak *et al*. (17) and others (64) have suggested that the gastrointestinal tract is a point of entry for a second pathogenic hit that goes on to affect the CNS. The double transgenic mice expressing mutant α-synucleins offer an opportunity to investigate the hypothesis that the early ENS dysfunction is not only an early marker of the disease, but also which, when triggered, facilitates the entry of deleterious factors that cause progression and spread to the CNS.

MATERIALS AND METHODS

Animals

Mice were given free access to food and drinking water. All animals were maintained at 24°C with 55% relative humidity on a 12-h light cycle (0700–1900-h). All animals were handled in accordance with the guidelines of NIH and University California, San Francisco Animal Care and Use Committee requirements.

Mutagenesis of RP1-27M07 PAC. The 145 kb PAC RP1-27M07 (BAC/PAC Resource Center, Children's Hospital, Oakland, CA, USA) with a human genomic DNA insert containing the human wild-type *SNCA* gene was described previously (65). We generated a transgenic mouse line carrying the wild-type *SNCA* gene (PAC-Tg($SNCA^{WT}$)) in a FVB/N background using standard pronuclear injection methods as described previously (35). This PAC-Tg($SNCA^{WT}$) transgenic line was crossed onto a previously described mouse line carrying a disrupted *Snca* gene ($Snca^{-/-}$) in a 129S6//SvEvTac background (34) and the resulting F1 generation was intercrossed to generate PAC-Tg($SNCA^{WT}$);$Snca^{-/-}$ in a mixed FVB/N × 129S6/background. The A53T and A30P mutations were introduced into the RP1-27M07 PAC by a two-step allelic exchange using recombineering in the *E. coli* strain DY380, which allows a heat-inducible expression of recombinase (32). A DNA construct consisting of a cassette containing chloramphenicol acetyltransferase and the *Bacillus subtilis* sacB gene flanked by ∼100 bp of the intron sequence flanking exon 3 (in which A30P mutation occurs) or exon 4 (in which the A53T mutation occurs) was electroporated into DY380 containing RP1-27M07. Following heat-shock to allow recombination to occur, recombinants were selected in chloramphenicol. To generate the construct for the second step of the allelic exchange, a genomic fragment containing exon 3 or exon 4, along with ∼100 bp of flanking intron sequence, was amplified by PCR using RP1-27M07 as template, cloned in pTarget (Promega, Fitchburg, WI, USA) and the A30P or A53T mutation was introduced by site-directed mutagenesis (Stratagene Quick-change mutagenesis kit). The PCR product was purified and electroporated into DY380 containing the PAC with the chloramphenicol resistance and *sacB* gene cassette and, following induction of recombinase, clones with the mutant exon 3 or 4 and lacking the cassette were selected by resistance to sucrose.

Generation of mice

Using standard pronuclear injection methods as described previously (35), we generated independent transgenic mouse lines carrying either the PAC-$SNCA^{A53T}$ (PAC-Tg($SNCA^{A53T}$)) or PAC-$SNCA^{A30P}$ (PAC-Tg($SNCA^{A30P}$)) mutant PACs in a FVB/N background. Two independent lines of founder mice for each construct expressing A53T or A30P α-synuclein and were capable of germline transmission were selected for

further analysis. Each of the PAC-Tg(*SNCA*^{A53T}) transgenic lines was crossed onto *Snca*$^{-/-}$ knock-out mice in a 129S6//SvEvTac background (34) and the resulting F1 generation was intercrossed to generate PAC-Tg(*SNCA*^{A53T});Snca$^{-/-}$ in a mixed FVB/N × 129S6/ background. The two independent PAC-Tg(*SNCA*^{A53T});Snca$^{-/-}$ lines were then bred together to create a line of double transgenic animals, dbl-PAC-Tg(*SNCA*^{A53T})$^{+/+}$;*Snca*$^{-/-}$, homozygous for both insertion sites of the PAC. Homozygosity for the PAC was determined by counting FISH signals using labeled RP1-27M07 on interphase nuclei in peripheral blood on slides. The PAC-Tg(*SNCA*^{A30P}) mice were similarly crossed onto the Snca$^{-/-}$ background and the two independent PAC-Tg(*SNCA*^{A30P});Snca$^{-/-}$ lines bred together to create double transgenic animals (dbl-PAC-Tg(*SNCA*^{A30P})$^{+/+}$;*Snca*$^{-/-}$) with both PAC-*SNCA*^{A30P} insertion sites. However, because one of the two PAC-*SNCA*^{A30P} lines carried its insertion on the X chromosome, only female dbl-PAC-Tg(*SNCA*^{A30P}) were homozygous for both PAC insertions (four copies of the PAC) whereas the males had three copies of the PAC (data not shown). As controls, we first bred the PAC-Tg(*SNCA*^{WT}) with *Snca* knock-out (*Snca*$^{-/-}$) mice, intercrossed the resulting F1 generation and selected a line homozygous for the *SNCA* PAC in which wild-type human *SNCA* was expressed without endogenous mouse protein PAC-Tg(*SNCA*^{WT})$^{+/+}$;*Snca*$^{-/-}$. Finally, we also crossed wild-type FVB/N with wild-type or *Snca* knock-out (*Snca*$^{-/-}$) 129S6//SvEvTac to create matched cohorts of *Snca*$^{+/+}$ or *Snca*$^{-/-}$ animals with mixed background similar to the PAC transgenic animals.

Polymerase chain reaction

Genotyping of mouse progeny was performed on tail genomic DNA by PCR using transgene-specific primer set (F: GGAA ACTTGGGTGGGAACTT; R: AGTTGGGGAGGAAGGA AGAA) or primers for the knockout allele described previously (34).

Fluorescence *in situ* hybridization

Interphase fluorescence *in situ* hybridization (FISH) was performed on blood samples obtained by submandibular bleeding for determination of transgene heterozygosity, homozygosity or double homozygosity (66). The FISH probe was generated from PAC RP1-27M07, which contains the whole human α-synuclein gene as well as 34 kb of sequence upstream of the first exon and was labeled with Cy3-dCTP (GE Healthcare PA-53021) using the BioPrime labeling kit (Invitrogen) following manufacturer's protocol. Cytogenetic and probe preparations, hybridization and detection were carried out following standard protocols with minor modifications (67,68). Samples were scored on a Nikon Eclipse E800.

Quantitative RT–PCR

The brain and descending colon were harvested from five individual mice per genotype all on the same day and stored in RNAlater (Qiagen). Tissues were collected in PBS (0.9% NaCl in 0.01 M sodium phosphate buffer, pH7.4) that had been treated with 0.1% diethyl pyrocarbonate (Sigma). The wall of the descending colon was opened, cleaned and mucosa removed. Total RNA was extracted using the RNeasy Lipid tissue kit (Qiagen) according to manufacturer's instructions including DNase treatment and stored at −80°C.

cDNA was prepared from 1 μg of total RNA by reverse transcription using random hexamer primers with the High-Capacity cDNA Reverse Transcription kit (Applied Biosystems Inc.) following manufacturer's instructions. Primers for amplification of cDNA encoding beta-actin (Forward: 5′-TGT TTG AGA CCT TCA ACA CC-3′ and Reverse: 5′-CAG TAA TCT CCT TCT GCA TCC-3′) were used to confirm cDNA quality.

Real time PCR was performed on the ABI PRISM 7900HT system by using TaqMan Gene Expression Master Mix (Applied Biosystems) with four Taqman Gene Expression assays: h*SNCA* (Hs00240906_m1), m*Snca* (Mm00447331_m1), synaptophysin (Mm00436850_m1) and *Elavl4*/HuD (Mm01263578_m1). Each probe was labeled with reporter dye FAM at 5′ end and a non-fluorescent quencher (TAMRA) linked to the 3′. The thermal cycler conditions were as follows: hold for 2 min at 50°C, 10 min at 95°C, followed by forty, two-step PCR cycles of 95°C for 30 s and 60°C for 1 min. The expression of h*SNCA* and m*Snca* were normalized to both synaptophysin and *Elavl4*, which are reference housekeeping genes not thought to be subject to regulation. The cycle number at which any particular sample crossed that threshold (C_t) was then used to determine fold difference; all the samples were measured in quadruplicate and averaged. Fold difference was calculated as $2^{\Delta C_t}$ where $\Delta C_t = [C_t(Syp) - C_t(SNCA)]$ or $2^{\Delta C_t}$ where $\Delta C_t = [C_t(Elavl4) - C_t(SNCA)]$ and the expression relative to endogenous mouse *Snca* calculated as $2^{\Delta\Delta C_t}$ where $\Delta\Delta C_t = \Delta C_t(SNCA) - \Delta C_t(Snca)$.

Western blotting

The presence of α-synuclein was assayed with mouse anti α-synuclein-specific (BD Transduction Laboratories) and rabbit anti-α-synuclein (Assay Designs) antibodies that recognize both human and mouse α-synuclein. Protein lysates from brain was prepared as previously described (34). Protein lysate from gut was prepared from segments of stomach, ileum, proximal and distal colon that were harvested and washed with PBS, the mucosa removed, and the remaining layers homogenized at 27 000 rpm using a Tissue Tearor (Biospec Products Inc.) in 20 mM Tris–HCl, pH 7.5,150 mM NaCl, 1% Triton X-100 in the presence of Protease Inhibitor Cocktail tablet (Roche). Total protein in lysates was determined by the BCA^{TM} Protein Assay kit (Pierce), mixed 1:1 (v/v) with Laemmli loading buffer and analyzed by western blotting (69). Bands were visualized with horseradish peroxidase-coupled goat anti-mouse or anti-rabbit IgG (GE Healthcare) and the chemiluminescent substrate ECL system used for detection (GE Healthcare Cell Signaling). α-Synuclein signals were normalized for gel loading using mouse anti α-tubulin or anti-β-actin (Calbiochem).

Immunocytochemistry

For brains, mice were anesthetized by intraperitoneal injection of Avertin, then intracardially perfused with 10 ml PBS/

heparin (10 μg/ml) followed by 70% ethanol/150 mM NaCl fixative. The brains were dissected out of the skull and post-fixed overnight 4°C in fresh fixative. Immunohistochemistry was performed as described previously (70).

For histological examination of the ENS, mice were euthanized and segments of stomach, ileum, proximal colon and distal colon were collected in PBS to which the muscle relaxant nicardipine (10^{-6} M; Sigma) had been added to prevent muscle spasm. The contents were flushed out with PBS and preparations cut open along the mesenteric border. For whole mounts, the tissue was stretched tautly and pinned flat on Sylgard 184 plates (Dow Corning) with the mucosal surface facing down. Specimens were fixed for 80 min at room temperature with 4% paraformaldehyde, pH 7.4/3% sucrose, rinsed in 3% sucrose/PBS then washed three times with PBS for a total of 30 min. The gastrointestinal tract was removed at University California; San Francisco, fixed (see above), and transported to Columbia University for additional analysis (Z.S.L and M.G.). Laminar preparations with adherent myenteric plexus (LMMP) and submucosa (containing the submucosal plexus, SMP) were prepared from the intestines of Dbl-PAC-Tg($SNCA^{A53T}$); Snca −/− and PAC($SNCA^{WT}$); Snca −/− mice by dissection of the gut wall and stained as previously described (59,60). The preparations were permeabilized with Triton X-100 (1% in PBS) for 1 h at room temperature and then digested with proteinase K (50 μg/ml in PBS) at 55° C for 1 h. Following digestion, non-specific staining was blocked with 10% normal horse serum and the specimens were incubated with sheep antibodies to human α-synuclein (diluted 1:250; Abcam, ab6162) for 48 h at room temperature. Sites of antibody binding were visualized with Alexa 594-labeled donkey antibodies to sheep immunoglobulin (diluted 1:200; 2 h, room temperature). Tissue was counterstained with bisbenzamide (1 μg/ml) to demonstrate DNA. As control for α-synuclein reactivity, ileal and colonic samples were prepared from $Snca^{-/-}$ mice in an identical manner and shown to have no immunoreactivity.

Motor tests

Motor tests were carried out in representative cohorts of three different ages (6, 12 and 18 months old), always at the same time of the day, using age-matched transgenic and control animals of both genders. Mice spent about an hour before the start of any experiments in the testing room to habituate. Variable numbers of mice were used and the exact number for each genotype for each test at each age point are given in the Supplementary Material, Tables S2 and S3. None of the measurements were done on fewer than 10 mice and most measurements were performed on ∼20–30 mice.

Rotarod test. The Ugo Basile rotarod was used to test mice motor ability as described previously (34). Mice were tested using four trials per day on three consecutive days. The rod accelerated from 4 to 40 rpm over 5 min and then remained at 40 rpm for an additional 5 min for each trial. During the trial, the time was recorded when the mice fell from the rod up to a maximum of 10 min. The mice rested 10 min between the trials.

Open field. Spontaneous motor activity was recorded over a period of 10 min by measuring horizontal and vertical interruption of infrared PhotoBeams in a 16 inch × 16 inch arena of the SmartFrame Open Field System (Kinder Scientific) using MotorMonitor software.

Dopamine and metabolite analysis

The brains of mice were rapidly removed and placed on ice-cooled plates for dissection of the substantia nigra, cortex, ventral tegmental area, hippocampus and striatum. Brains were removed at University California; San Francisco, dissected and weighed and transported to St. Jude Children's Research Hospital for metabolite analysis. Tissues were processed and assayed by HPLC as previously described (71).

Cell counting

For examination of cell number, mice were processed and analyzed as previously reported (72) by using the optical fractionator (73) on a Bioquant Image Analysis System (R&M Biometrics, Nashville, TN, USA).

Olfactory testing

Novel odor test. A cotton tipped applicator (Q-tip) was dipped in vanilla extract and taped to the lid of a clean cage. The time each mouse spent sniffing was recorded (74).

Buried food test. Mice were fasted overnight. Each test mouse was placed in the center of a clean mouse cage and one Froot Loop (Kellogg's) was buried under ∼1 cm of bedding in one corner of the cage. The time spent for each mouse to find the Froot Loop and start eating it was recorded (75).

Gastrointestinal function testing

Variable numbers of mice were used for the different tests; exact numbers of mice of each genotype for each test at different ages are given in the Supplementary Material, Tables S4–S6. Except for a few of the earliest time points in Supplementary Material, Table S5, all measurements were done on more than 10 mice and most measurements were performed with between ∼20 and 30 mice.

Stool weight. Total stool weight was measured by placing the animals in a novel environment and collecting all stool produced over a 1 h time period at the same time of day (10–11 AM). Stool was then dessicated at 75°C overnight to determine dry weight. Stool water is the difference between these two measurements.

Colonic motility. Colonic motility was measured by the bead expulsion test as previously described (39). Briefly, a glass bead (diameter, 3 mm) was inserted through the anus and pushed, with a polished glass rod, into the colon for a distance of 2 cm (75). The time required for expulsion of the glass bead was recorded.

Whole gut transit time. WGTT was measured by oral gavage of 0.3 ml of 6% (w/v) carmine dye in 0.5% methylcellulose (Sigma) to each mouse as previously described (76). The time taken from the administration of carmine until the first appearance of one red pellet was recorded. The observation was performed for 12 h after the administration of carmine. Animals whose stool had no dye even after 12 h were recorded as >12 h.

Statistical analysis

A non-parametric two-tailed Mann–Whitney *U* test was used to determine statistical significance when the data were not normally distributed or could only be ranked. Student's *t*-test was used otherwise. All data were analyzed by GraphPad Prism 4.0 statistical software (GraphPad Software, Inc., San Diego, CA, USA).

In vivo electrocardiogram telemetry collection

For long-term electrocardiogram (ECG) recording, adult mice were anesthetized with isoflurane (five each of *Snca*−/− and Dbl-PAC-Tg($SNCA^{A53T}$)$^{+/+}$;*Snca*−/−). A midline incision was made on the back along the spine to insert a telemetric transmitter (TA10EA-F20, Data Sciences International; St. Paul, MN, USA) into a subcutaneous pocket with paired wire electrodes placed over the thorax (chest bipolar ECG lead). Mice were allowed to recover for 72 h post-surgery before ECG data were collected. Measurements were collected in unanesthetized animals during nocturnal and diurnal activity over at 24 h per ECG trace. Experiments were initiated at least 36 h after recovery from surgical implantation. Mice were housed in individual cages with free access to food and water and were exposed to 12-h light/dark cycles in a thermostatically controlled room. ECG signals were computer-recorded with the use of a telemetry receiver and an analog-to-digital conversion data acquisition system for display and analysis by Dataquest A.R.T. 2.3 software (Data Sciences International). Mean heart rate values were obtained in each mouse for an overall 24-h period including both the light and dark cycles in the room housing the rodents. ECG parameters were measured at a fixed RR interval of 100 ms and HRV Spectrum analyses were performed with Chart 5 software, with manual verification. P duration, RR intervals PR interval duration, QRS interval duration, QT_C interval duration, JT interval duration and heart rate variability were measured.

SUPPLEMENTARY MATERIAL

Supplementary Material is available at *HMG* online.

ACKNOWLEDGEMENTS

We thank Deborah Cabin for samples of spinal cord containing SDS-resistant synuclein aggregates and Jeffrey Olgin for helpful discussions on heart rate analysis. We also thank Dr Nigel Killeen and the UCSF Helen Diller Family Comprehensive Cancer Center Transgenic/Targeted Mutagenesis core with ooccyte injection services for creating transgenic mice.

Conflict of Interest statement. None declared.

FUNDING

Supported by the Division of Intramural Research, National Human Genome Research Institute (NIH), a grant from the Michael J. Fox Foundation, and institutional funding from the UCSF Department of Medicine and Institute of Human Genetics (R.L.N.), National Institutes of Health (grant number NS053488) (B.G.), American Lebanese Syrian Associated Charities (R.S.) and National Institutes of Health (grant numbers NS12969 and NS15547) (M.G.).

REFERENCES

1. Nussbaum, R.L. and Ellis, C.E. (2003) Alzheimer's disease and Parkinson's disease. *N. Engl. J. Med.*, **348**, 1356–1364.
2. Braak, H., Del Tredici, K., Bratzke, H., Hamm-Clement, J., Sandmann-Keil, D. and Rub, U. (2002) Staging of the intracerebral inclusion body pathology associated with idiopathic Parkinson's disease (preclinical and clinical stages). *J. Neurol.*, **249** (Suppl. 3), III/1–5.
3. Halliday, G.M., Del Tredici, K. and Braak, H. (2006) Critical appraisal of brain pathology staging related to presymptomatic and symptomatic cases of sporadic Parkinson's disease. *J. Neural. Transm. Suppl.*, **70**, 99–103.
4. Braak, H., Ghebremedhin, E., Rub, U., Bratzke, H. and Del Tredici, K. (2004) Stages in the development of Parkinson's disease-related pathology. *Cell Tissue Res.*, **318**, 121–134.
5. Wolters, E. and Braak, H. (2006) Parkinson's disease: premotor clinico-pathological correlations. *J. Neural. Transm. Suppl.*, 309–319.
6. Djaldetti, R., Lev, N. and Melamed, E. (2009) Lesions outside the CNS in Parkinson's disease. *Mov. Disord.*, **24**, 793–800.
7. Pfeiffer, R.F. (2003) Gastrointestinal dysfunction in Parkinson's disease. *Lancet. Neurol.*, **2**, 107–116.
8. Jost, W.H. and Eckardt, V.F. (2003) Constipation in idiopathic Parkinson's disease. *Scand. J. Gastroenterol.*, **38**, 681–686.
9. Jost, W.H. (2010) Gastrointestinal dysfunction in Parkinson's Disease. *J. Neurol. Sci.*, **289**, 69–73.
10. Natale, G., Pasquali, L., Ruggieri, S., Paparelli, A. and Fornai, F. (2008) Parkinson's disease and the gut: a well known clinical association in need of an effective cure and explanation. *Neurogastroenterol. Motil.*, **20**, 741–749.
11. Abbott, R.D., Petrovitch, H., White, L.R., Masaki, K.H., Tanner, C.M., Curb, J.D., Grandinetti, A., Blanchette, P.L., Popper, J.S. and Ross, G.W. (2001) Frequency of bowel movements and the future risk of Parkinson's disease. *Neurology*, **57**, 456–462.
12. Ashraf, W., Pfeiffer, R.F., Park, F., Lof, J. and Quigley, E.M. (1997) Constipation in Parkinson's disease: objective assessment and response to psyllium. *Mov. Disord.*, **12**, 946–951.
13. Shults, C.W. (2006) Lewy bodies. *Proc. Natl. Acad. Sci. USA*, **103**, 1661–1668.
14. Braak, H. and Del Tredici, K. (2009) Neuroanatomy and pathology of sporadic Parkinson's disease. *Adv. Anat. Embryol. Cell Biol.*, **201**, 1–119.
15. Edwards, L.L., Quigley, E.M. and Pfeiffer, R.F. (1992) Gastrointestinal dysfunction in Parkinson's disease: frequency and pathophysiology. *Neurology*, **42**, 726–732.
16. Lebouvier, T., Chaumette, T., Damier, P., Coron, E., Touchefeu, Y., Vrignaud, S., Naveilhan, P., Galmiche, J.P., Bruley des Varannes, S., Derkinderen, P. *et al.* (2008) Pathological lesions in colonic biopsies during Parkinson's disease. *Gut*, **57**, 1741–1743.
17. Braak, H., de Vos, R.A., Bohl, J. and Del Tredici, K. (2006) Gastric alpha-synuclein immunoreactive inclusions in Meissner's and Auerbach's plexuses in cases staged for Parkinson's disease-related brain pathology. *Neurosci. Lett.*, **396**, 67–72.
18. Gasser, T. (2007) Update on the genetics of Parkinson's disease. *Mov. Disord.*, **22** (Suppl. 17), S343–S350.
19. Polymeropoulos, M.H., Lavedan, C., Leroy, E., Ide, S.E., Dehejia, A., Dutra, A., Pike, B., Root, H., Rubenstein, J., Boyer, R. *et al.* (1997) Mutation in the alpha-synuclein gene identified in families with Parkinson's disease. *Science*, **276**, 2045–2047.

20. Kruger, R., Kuhn, W., Muller, T., Woitalla, D., Graeber, S., Kosel, S., Przuntek, H., Epplen, J.T., Schols, L. and Riess, O. (1998) Ala30Pro mutation in the gene encoding alpha-synuclein in Parkinson's disease. *Nat. Genet.*, **18**, 106–108.
21. Singleton, A.B., Farrer, M., Johnson, J., Singleton, A., Hague, S., Kachergus, J., Hulihan, M., Peuralinna, T., Dutra, A., Nussbaum, R. *et al.* (2003) alpha-Synuclein locus triplication causes Parkinson's disease. *Science*, **302**, 841.
22. Chartier-Harlin, M.C., Kachergus, J., Roumier, C., Mouroux, V., Douay, X., Lincoln, S., Levecque, C., Larvor, L., Andrieux, J., Hulihan, M. *et al.* (2004) Alpha-synuclein locus duplication as a cause of familial Parkinson's disease. *Lancet*, **364**, 1167–1169.
23. Zarranz, J.J., Alegre, J., Gomez-Esteban, J.C., Lezcano, E., Ros, R., Ampuero, I., Vidal, L., Hoenicka, J., Rodriguez, O., Atares, B. *et al.* (2004) The new mutation, E46K, of alpha-synuclein causes Parkinson and Lewy body dementia. *Ann. Neurol.*, **55**, 164–173.
24. Mezey, E., Dehejia, A.M., Harta, G., Suchy, S.F., Nussbaum, R.L., Brownstein, M.J. and Polymeropoulos, M.H. (1998) Alpha synuclein is present in Lewy bodies in sporadic Parkinson's disease. *Mol. Psychiatry.*, **3**, 493–496.
25. Tofaris, G.K., Razzaq, A., Ghetti, B., Lilley, K.S. and Spillantini, M.G. (2003) Ubiquitination of alpha-synuclein in Lewy bodies is a pathological event not associated with impairment of proteasome function. *J. Biol. Chem.*, **278**, 44405–44411.
26. Spillantini, M.G., Schmidt, M.L., Lee, V.M.Y., Trojanowski, J.Q., Jakes, R. and Goedert, M. (1997) alpha-Synuclein in Lewy bodies. *Nature*, **388**, 839–840.
27. Chesselet, M.F. (2008) In vivo alpha-synuclein overexpression in rodents: a useful model of Parkinson's disease? *Exp. Neurol.*, **209**, 22–27.
28. Meredith, G.E., Sonsalla, P.K. and Chesselet, M.F. (2008) Animal models of Parkinson's disease progression. *Acta Neuropathol.*, **115**, 385–398.
29. Terzioglu, M. and Galter, D. (2008) Parkinson's disease: genetic versus toxin-induced rodent models. *Febs. J.*, **275**, 1384–1391.
30. Melrose, H.L., Lincoln, S.J., Tyndall, G.M. and Farrer, M.J. (2006) Parkinson's disease: a rethink of rodent models. *Exp. Brain Res.*, **173**, 196–204.
31. Jost, W.H. (1997) Gastrointestinal motility problems in patients with Parkinson's disease. Effects of antiparkinsonian treatment and guidelines for management. *Drugs Aging*, **10**, 249–258.
32. Liu, P., Jenkins, N.A. and Copeland, N.G. (2003) A highly efficient recombineering-based method for generating conditional knockout mutations. *Genome Res.*, **13**, 476–484.
33. Cabin, D.E., Gispert-Sanchez, S., Murphy, D., Auburger, G., Myers, R.R. and Nussbaum, R.L. (2005) Exacerbated synucleinopathy in mice expressing A53T SNCA on a Snca null background. *Neurobiol. Aging*, **26**, 25–35.
34. Cabin, D.E., Shimazu, K., Murphy, D., Cole, N.B., Gottschalk, W., McIlwain, K.L., Orrison, B., Chen, A., Ellis, C.E., Paylor, R. *et al.* (2002) Synaptic vesicle depletion correlates with attenuated synaptic responses to prolonged repetitive stimulation in mice lacking alpha-synuclein. *J. Neurosci.*, **22**, 8797–8807.
35. Gispert, S., Del Turco, D., Garrett, L., Chen, A., Bernard, D.J., Hamm-Clement, J., Korf, H.W., Deller, T., Braak, H., Auburger, G. *et al.* (2003) Transgenic mice expressing mutant A53T human alpha-synuclein show neuronal dysfunction in the absence of aggregate formation. *Mol. Cell. Neurosci.*, **24**, 419–429.
36. Braak, H., Tredici, K.D., Rub, U., de Vos, R.A., Jansen Steur, E.N. and Braak, E. (2003) Staging of brain pathology related to sporadic Parkinson's disease. *Neurobiol. Aging*, **24**, 197–211.
37. Degen, L.P. and Phillips, S.F. (1996) How well does stool form reflect colonic transit? *Gut*, **39**, 109–113.
38. Hammer, J. and Phillips, S.F. (1993) Fluid loading of the human colon: effects on segmental transit and stool composition. *Gastroenterology*, **105**, 988–998.
39. Chen, J.J., Li, Z., Pan, H., Murphy, D.L., Tamir, H., Koepsell, H. and Gershon, M.D. (2001) Maintenance of serotonin in the intestinal mucosa and ganglia of mice that lack the high-affinity serotonin transporter: abnormal intestinal motility and the expression of cation transporters. *J. Neurosci.*, **21**, 6348–6361.
40. Cali, R.L., Blatchford, G.J., Perry, R.E., Pitsch, R.M., Thorson, A.G. and Christensen, M.A. (1992) Normal variation in anorectal manometry. *Dis. Colon Rectum*, **35**, 1161–1164.
41. Doty, R.L., Stern, M.B., Pfeiffer, C., Gollomp, S.M. and Hurtig, H.I. (1992) Bilateral olfactory dysfunction in early stage treated and untreated idiopathic Parkinson's disease. *J. Neurol. Neurosurg. Psychiatry*, **55**, 138–142.
42. Haapaniemi, T.H., Pursiainen, V., Korpelainen, J.T., Huikuri, H.V., Sotaniemi, K.A. and Myllyla, V.V. (2001) Ambulatory ECG and analysis of heart rate variability in Parkinson's disease. *J. Neurol. Neurosurg. Psychiatry*, **70**, 305–310.
43. Singleton, A., Gwinn-Hardy, K., Sharabi, Y., Li, S.T., Holmes, C., Dendi, R., Hardy, J., Crawley, A. and Goldstein, D.S. (2004) Association between cardiac denervation and parkinsonism caused by alpha-synuclein gene triplication. *Brain*, **127**, 768–772.
44. Thireau, J., Zhang, B.L., Poisson, D. and Babuty, D. (2008) Heart rate variability in mice: a theoretical and practical guide. *Exp. Physiol.*, **93**, 83–94.
45. Scherzer, C.R., Grass, J.A., Liao, Z., Pepivani, I., Zheng, B., Eklund, A.C., Ney, P.A., Ng, J., McGoldrick, M., Mollenhauer, B. *et al.* (2008) GATA transcription factors directly regulate the Parkinson's disease-linked gene alpha-synuclein. *Proc. Natl. Acad. Sci. USA*, **105**, 10907–10912.
46. Chiba-Falek, O. and Nussbaum, R.L. (2001) Effect of allelic variation at the NACP-Rep1 repeat upstream of the alpha-synuclein gene (SNCA) on transcription in a cell culture luciferase reporter system. *Hum. Mol. Genet.*, **10**, 3101–3109.
47. Wang, L., Fleming, S.M., Chesselet, M.F. and Tache, Y. (2008) Abnormal colonic motility in mice overexpressing human wild-type alpha-synuclein. *Neuroreport*, **19**, 873–876.
48. Jost, W.H., Jung, G. and Schimrigk, K. (1994) Colonic transit time in nonidiopathic Parkinson's syndrome. *Eur. Neurol.*, **34**, 329–331.
49. Abbott, R.D., Ross, G.W., Petrovitch, H., Tanner, C.M., Davis, D.G., Masaki, K.H., Launer, L.J., Curb, J.D. and White, L.R. (2007) Bowel movement frequency in late-life and incidental Lewy bodies. *Mov. Disord.*, **22**, 1581–1586.
50. Golbe, L.I., Di Iorio, G., Bonavita, V., Miller, D.C. and Duvoisin, R.C. (1990) A large kindred with autosomal dominant Parkinson's disease. *Ann. Neurol.*, **27**, 276–282.
51. Kruger, R., Kuhn, W., Leenders, K.L., Sprengelmeyer, R., Muller, T., Woitalla, D., Portman, A.T., Maguire, R.P., Veenma, L., Schroder, U. *et al.* (2001) Familial parkinsonism with synuclein pathology: Clinical and PET studies of A30P mutation carriers. *Neurology*, **56**, 1355–1362.
52. Braak, H. and Del Tredici, K. (2008) Invited Article: nervous system pathology in sporadic Parkinson disease. *Neurology*, **70**, 1916–1925.
53. Singaram, C., Ashraf, W., Gaumnitz, E.A., Torbey, C., Sengupta, A., Pfeiffer, R. and Quigley, E.M. (1995) Dopaminergic defect of enteric nervous system in Parkinson's disease patients with chronic constipation. *Lancet*, **346**, 861–864.
54. Wakabayashi, K., Takahashi, H., Ohama, E., Takeda, S. and Ikuta, F. (1993) Lewy bodies in the visceral autonomic nervous system in Parkinson's disease. *Adv. Neurol.*, **60**, 609–612.
55. Attems, J. and Jellinger, K.A. (2008) The dorsal motor nucleus of the vagus is not an obligatory trigger site of Parkinson's disease. *Neuropathol. Appl. Neurobiol.*, **34**, 466–467.
56. Kalaitzakis, M.E., Graeber, M.B., Gentleman, S.M. and Pearce, R.K. (2008) Controversies over the staging of alpha-synuclein pathology in Parkinson's disease. *Acta. Neuropathol.*, **116**, 125–128. author reply 129–131.
57. Parkkinen, L., Pirttila, T. and Alafuzoff, I. (2008) Applicability of current staging/categorization of alpha-synuclein pathology and their clinical relevance. *Acta. Neuropathol.*, **115**, 399–407.
58. Rakshi, J.S., Uema, T., Ito, K., Bailey, D.L., Morrish, P.K., Ashburner, J., Dagher, A., Jenkins, I.H., Friston, K.J. and Brooks, D.J. (1999) Frontal, midbrain and striatal dopaminergic function in early and advanced Parkinson's disease A 3D [(18)F]dopa-PET study. *Brain*, **122**, 1637–1650.
59. Li, Z.S., Schmauss, C., Cuenca, A., Ratcliffe, E. and Gershon, M.D. (2006) Physiological modulation of intestinal motility by enteric dopaminergic neurons and the D2 receptor: analysis of dopamine receptor expression, location, development, and function in wild-type and knock-out mice. *J. Neurosci.*, **26**, 2798–2807.
60. Li, Z.S., Pham, T.D., Tamir, H., Chen, J.J. and Gershon, M.D. (2004) Enteric dopaminergic neurons: definition, developmental lineage, and effects of extrinsic denervation. *J. Neurosci.*, **24**, 1330–1339.

61. Anderson, G., Noorian, A.R., Taylor, G., Anitha, M., Bernhard, D., Srinivasan, S. and Greene, J.G. (2007) Loss of enteric dopaminergic neurons and associated changes in colon motility in an MPTP mouse model of Parkinson's disease. *Exp. Neurol.*, **207**, 4–12.
62. Phillips, R.J., Walter, G.C., Wilder, S.L., Baronowsky, E.A. and Powley, T.L. (2008) Alpha-synuclein-immunopositive myenteric neurons and vagal preganglionic terminals: autonomic pathway implicated in Parkinson's disease? *Neuroscience*, **153**, 733–750.
63. Lee, M.K., Stirling, W., Xu, Y., Xu, X., Qui, D., Mandir, A.S., Dawson, T.M., Copeland, N.G., Jenkins, N.A. and Price, D.L. (2002) Human alpha-synuclein-harboring familial Parkinson's disease-linked Ala- 53 –> Thr mutation causes neurodegenerative disease with alpha-synuclein aggregation in transgenic mice. *Proc. Natl. Acad. Sci. USA*, **99**, 8968–8973.
64. Jang, H., Boltz, D., Sturm-Ramirez, K., Shepherd, K.R., Jiao, Y., Webster, R. and Smeyne, R.J. (2009) Highly pathogenic H5N1 influenza virus can enter the central nervous system and induce neuroinflammation and neurodegeneration. *Proc. Natl. Acad. Sci. USA*, **106**, 14063–14068.
65. Touchman, J.W., Dehejia, A., Chiba-Falek, O., Cabin, D.E., Schwartz, J.R., Orrison, B.M., Polymeropoulos, M.H. and Nussbaum, R.L. (2001) Human and mouse alpha-synuclein genes: comparative genomic sequence analysis and identification of a novel gene regulatory element. *Genome Res.*, **11**, 78–86.
66. Dinchuk, J.E., Kelley, K. and Boyle, A.L. (1994) Fluorescence in situ hybridization of interphase nuclei isolated from whole blood of transgenic mice. *Biotechniques*, **17**, 954–961.
67. Gribnau, J., Hochedlinger, K., Hata, K., Li, E. and Jaenisch, R. (2003) Asynchronous replication timing of imprinted loci is independent of DNA methylation, but consistent with differential subnuclear localization. *Genes Dev.*, **17**, 759–773.
68. Sambrook, J., Fritsch, E.F. and Maniatis, T. (1989) *Molecular Cloning: A Laboratory Manual*. Cold Spring Harbor Laboratory, Cold Spring Harbor, NY.
69. Gallagher, S.R., Ausubel, F.M., Brent, R., Kingston, R.E., Moore, D.D., Seidman, J.G., Smith, J.A. and Struhl, K. (eds) (2006) *Current Protocols in Molecular Biology*, John Wiley & Sons, Inc, pp. 10.12A.11–10.12A.37.
70. Waxman, E.A., Duda, J.E. and Giasson, B.I. (2008) Characterization of antibodies that selectively detect alpha-synuclein in pathological inclusions. *Acta Neuropathol.*, **116**, 37–46.
71. Smeyne, M., Boyd, J., Raviie Shepherd, K., Jiao, Y., Pond, B.B., Hatler, M., Wolf, R., Henderson, C. and Smeyne, R.J. (2007) GSTpi expression mediates dopaminergic neuron sensitivity in experimental parkinsonism. *Proc. Natl. Acad. Sci. USA*, **104**, 1977–1982.
72. Smeyne, M., Jiao, Y., Shepherd, K.R. and Smeyne, R.J. (2005) Glia cell number modulates sensitivity to MPTP in mice. *Glia*, **52**, 144–152.
73. West, M.J., Slomianka, L. and Gundersen, H.J. (1991) Unbiased stereological estimation of the total number of neurons in the subdivisions of the rat hippocampus using the optical fractionator. *Annat Rec*, **231**, 482–497.
74. Crawley, J. (2007) *What's Wrong with my Mouse?*, Wiley-Liss, New York.
75. Osinki, M.A., Bass, P. and Gaumnitz, E.A. (1999) Peripheral and central actions of orphanin FQ (nociceptin) on murine colon. *Am. J. Physiol. Cell. Physiol.*, **276**, G125–G131.
76. Nagakura, Y., Naitoh, Y., Kamato, T., Yamano, M. and Miyata, K. (1996) Compounds possessing 5-HT3 receptor antagonistic activity inhibit intestinal propulsion in mice. *Eur. J. Pharmacol.*, **311**, 67–72.